

Can kynurenic acid cause myelin loss in chicken optic nerves?

by

Akshay Gurdita

A thesis

presented to the University of Waterloo

in fulfillment of the

thesis requirement for the degree of

Masters of Science

in

Vision Science and Biology

Waterloo, Ontario, Canada, 2017

©Akshay Gurdita 2017

Author's Declaration

I hereby declare that I am the sole author of this thesis. This is a true copy of the thesis, including any required final revisions, as accepted by my examiners. I understand that my thesis may be made electronically available to the public.

Abstract

Kynurenic acid (KYNA) is one of many kynurenine intermediate products in the tryptophan metabolism pathway and has been shown to have neuro-activity. Previous work revealed that prolonged infusion of a high dose of KYNA could effectively reduce the myelin content in the rat spinal cord. We hypothesize that prolonged subdural infusion of kynurenic acid (KYNA) induces myelin loss in the optic nerves of chickens.

Seven day old *gallus gallus domesticus* chickens were randomly selected for infusion of 50 mM KYNA or phosphate buffered saline (PBS). KYNA or PBS were loaded into an osmotic pump that was attached to a catheter. The catheter was inserted into the optic nerve and the pump was implanted under the skin in upper back region of the bird. A third group of birds received no treatment. Electron micrographs were collected and the percent of myelinated axons, g-ratios, the number of astrocytes, and the axon diameters were calculated by sampling from 4 quadrants of optic nerve sections. Enzyme-linked immunosorbent assays (ELISA) were performed on serum from the three groups in order to determine differences in the level of myelin proteins myelin basic protein (MBP) and proteolipid protein (PLP). Semi-quantitative analysis of western blots was performed for myelin proteins: MBP, PLP, and myelin associated glycoprotein (MAG) in addition to glial fibrillary acidic protein (GFAP). A 2x3 mixed model analysis of variance (ANOVA) was used to determine differences between the three treatment groups and eyes. Count data were analyzed using two one-way Kruskal-Wallis ANOVAs.

Electron microscopy revealed that KYNA-infused nerves exhibited widespread loss of myelin sheaths and astrogliosis without inflammatory infiltration of the nerve. G-ratios for KYNA-infused chicks were greater than those for negative control birds (0.86 ± 0.04 for KYNA vs 0.78 ± 0.02 for NC; $p = 0.0029$) but were not significantly greater than compared to PBS-infused chicks (0.83 ± 0.06 ; $p = 0.2605$). ELISAs revealed no differences in the concentration of serum MBP or PLP across the three treatment groups indicating a non-destructive effect on myelin in the nerve ($p = 0.8330$ and $p = 0.8759$, respectively). Lastly, western blots revealed a qualitative reduction in the level of MBP and PLP, and GFAP in KYNA-infused birds compared to PBS-infused or negative control birds.

Subdural infusion of 50 mM KYNA for 7 days induces myelin loss without inflammatory infiltration in the chicken optic nerve. KYNA may be useful for illuminating mechanisms in myelin production or oligodendrocyte function.

Acknowledgements

I would like to thank my supervisor, Dr. Choh for all her guidance and support without which this work would not have been possible. I would also like to thank all of the graduate students in vision science and the department for their support. I would like to thank Nancy Gibson and Kathy Delaney for their help with animal handling and advice. Thank you to Miriam Heynen and Kevin vanDoorn for all of their help in the lab and technical expertise. If not for their help I would have never been able to complete my western blots. I would also like to thank Marcia Reid for embedding and sectioning the electron microscopy samples. Thank you to Varadhu Jayakumar for allowing me to borrow his SLR camera for imaging my western blots. I am grateful for the financial support from the government of Ontario for the Queen Elizabeth II Graduate Scholarship in Science and Technology and from the Natural Science and Engineering Research Council for the Canada Graduate Scholarship-Masters and the University of Waterloo for various scholarships and awards.

Table of Contents

Author's Declaration	ii
Abstract	iii
Acknowledgements	v
Table of Contents	vi
List of Figures	viii
List of Tables	ix
List of Abbreviations	x
I : LITERATURE REVIEW	1
1.1 The nervous system	1
1.1.1 Development of the nervous system	2
1.1.2 Central nervous system	4
1.1.3 Peripheral nervous system	5
1.1.4 Regeneration of the nervous system	5
1.2 The eye and optic nerve	10
1.2.1 Development of the eye and optic nerve	11
1.2.2 Diseases of the optic nerve	15
1.2.3 Optic nerve regeneration	18
1.3 The chick model	20
1.3.1 Anatomical differences of the chick retina and optic nerve	20
1.3.2 Optic nerve damage studies in chicks	21
1.4 Kynurenic acid	22
1.4.1 The kynurenine metabolic pathway	22
1.4.2 Kynurenines in neurological diseases	24
1.5 Drug delivery to the optic nerve	26
II : INTRODUCTION	29
III : MATERIAL AND METHODS	30
3.1 Animals	30

3.2 Implantation	30
3.2.1 Validation of the implantation technique.....	32
3.3 Histology and electron microscopy.....	32
3.3.1 Axon counts and g-ratios	33
3.4 Western blots and ELISAs	34
3.5 Statistical analysis	38
IV : RESULTS	39
4.1 Histology and electron microscopy.....	39
4.2 ELISA and western blots.....	40
V : DISCUSSION	48
LETTERS OF COPYRIGHT PERMISSIONS	55
FIGURE I-3.....	55
FIGURE I-4.....	56
FIGURE I-6.....	57
FIGURE I-8.....	58
REFERENCES	59

List of Figures

Figure I-1. Structure of a typical neuron.....	1
Figure I-2. Embryonic development of the vertebrate nervous system.....	3
Figure I-3. Regenerative process in the PNS.....	6
Figure I-4. Injury of axons in the CNS leads to the formation of a glial scar.....	7
Figure I-5. Anatomy of the human eye.....	10
Figure I-6. Development of the vertebrate eye.....	12
Figure I-7. 3-D block of a human retina.....	14
Figure I-8. Kynurenine metabolic pathway.....	23
Figure III-1. Illustration describing the surgical procedure with images indicating exposure of the optic nerve and catheter insertion.....	31
Figure III-2. Validation of the implant procedure.....	33
Figure III-3. EM image analysis method.....	34
Figure IV-1. Morphology and features of the normal chicken optic nerve.....	41
Figure IV-2. Effect of subdural infusion on the implanted and contralateral optic nerves for PBS-infused chicks.....	42
Figure IV-3. Effect of subdural infusion on the implanted and contralateral optic nerves for KYNA-infused chicks.....	43
Figure IV-4. Mean percent of myelinated axons (A,) and mean g-ratios (B) for negative control (NC), PBS-infused and KYNA-infused birds.....	44
Figure IV-5. Mean axon diameter (A) and mean number of astrocytes (B) for both eyes across negative control (NC), PBS-infused, and KYNA-infused birds.....	45
Figure IV-6. Semi-quantitative analysis of western blots data.....	47

List of Tables

Table III-1. Primary and secondary antibodies used for western blot analysis.	37
Table IV-1. Mean serum concentrations of PLP1 and MBP for KYNA-treated, PBS-treated and negative control birds.	46

List of Abbreviations

α 7nACh	α 7 nicotinic acetylcholine receptor
3-HANA	3-hydroxyanthranilic acid
3-HANAO	3-Hydroxyanthranilic acid oxygenase
3-HK	3-hydroxykynurenine
ANS	autonomic nervous system
bFGF	basic fibroblast growth factor
BDNF	brain-derived growth factor
CNS	central nervous system
CSF	cerebrospinal fluid
CSPGs	chondroitin sulphate proteoglycans
CNTF	ciliary neurotrophic factor
cAMP	cyclic adenine monophosphate
ELISA	Enzyme-linked immunosorbent assay
FGF	fibroblast growth factor
GCL	ganglion cell layer
GFAP	glial fibrillary acidic protein
GDNF	glial-derived neurotrophic factor
GPR35	G-protein-coupled receptor 35
GM-CSF	granulocyte-macrophage colony stimulating factor
HGF	hepatocyte growth factor
IS	inflammatory stimulation
INL	inner nuclear layer
IPL	inner plexiform layer
ION	ischemic optic neuropathy
KYNA	kynurenic acid
KATs	kynurenine aminotransferases
LGN	lateral geniculate nucleus
LIF	leukemia inhibitory factor
L-KYN	L-kynurenine
MS	multiple sclerosis
MAI	myelin associated inhibitor
MBP	myelin basic protein
MOG	myelin oligodendrocyte glycoprotein
P ₀	myelin protein zero
MAG	myelin-associated glycoprotein
NFL	nerve fiber layer
NGF	nerve growth factor
NT-3	neurotrophin 3
NT-4/5	neurotrophin 4/5

NAD ⁺	nicotinamide adenine dinucleotide
NgR	nogo receptor
NgR1	nogo-66 receptor
ONL	outer nuclear layer
OPL	outer plexiform layer
PNS	peripheral nervous system
PLP1	proteolipid protein-1
QUIN	quinolinic acid
RGC	retinal ganglion cell
SNS	somatic nervous system

I: LITERATURE REVIEW

1.1 The nervous system

The functional unit of the nervous system is a cell called a neuron (Figure I-1). A neuron consists of a cell body, dendrites and axon (Ramón y Cajal; Nolte, 2009). Neurons can communicate with each other by first sending electrical signals down the length of their axons (Hodgkin and Huxley, 1952; Nolte, 2009). At the end of the axon, neurotransmitters are released into the synaptic space between the end of the axon and the tip of the dendrite (Hodgkin and Huxley, 1952; Nolte, 2009). Neurotransmitters received at the post synaptic membrane, as a chemical signal, are converted back into an electrical signal which travels through the neuron and axon again (Hodgkin and Huxley, 1952; Nolte, 2009). Different types of neurons can

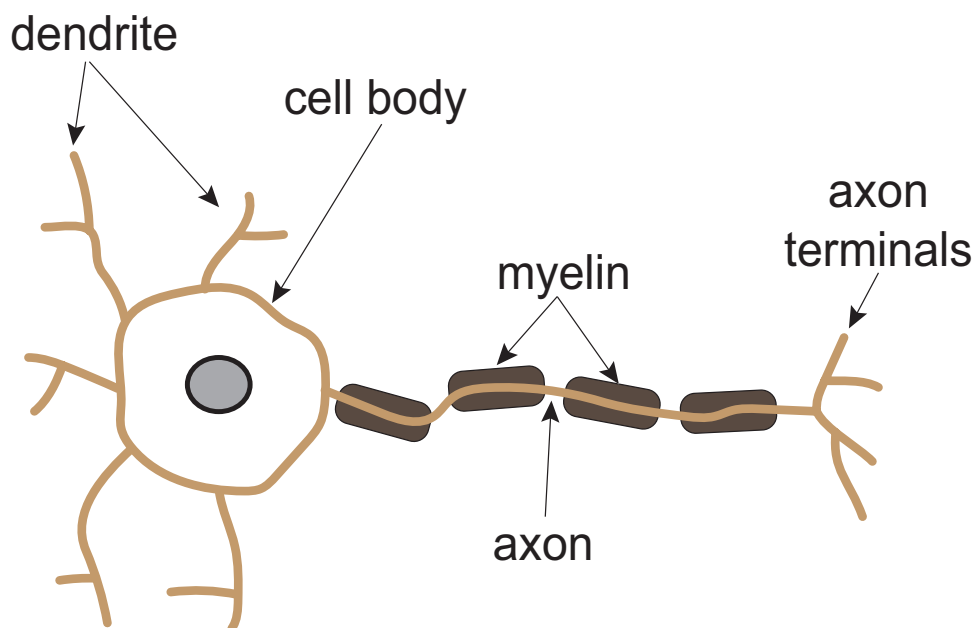


Figure I-1. Structure of a typical neuron. A neuron consists of the cell body, dendrites, axon and axon terminals. Dendrites receive signals from other neurons. The signal is passed down the cell body and axon and transmitted to other neurons through the axon terminals. Myelin wrapped around the axon insulates the electrical signal and increases the speed of transmission.

respond to unique modalities of stimuli and regulate different processes by sending signals to or from the brain (Nolte, 2009). For example, sensory neurons can respond to light, sound, odor, taste, pressure and heat and send messages to the brain (Nolte, 2009). Motor neurons transmit messages from the brain to control voluntary and involuntary movement (Nolte, 2009). In addition to neurons, non-neuronal cells called glial cells, provide support, nutrition, maintain homeostasis, form myelin, and participate in signal transmission in the nervous system (Nolte, 2009).

The vertebrate nervous system consists of the central nervous system (CNS) and the peripheral nervous system (PNS). The CNS consists of the brain and spinal cord while the PNS consists of the nerves and ganglia outside of the brain and spinal cord (Nolte, 2009).

1.1.1 Development of the nervous system

Development of the vertebrate nervous system begins during the third week of embryonic development (Nolte, 2009). In response to signals released from the midline mesoderm, a longitudinal band of ectoderm thickens, forming the neural plate (Nolte, 2009; Figure I-2A). The neural plate folds inward to form the neural groove, flanked by parallel neural folds (Nolte, 2009), which approach each other in the dorsal midline as the neural groove deepens. By the end of the third week, the neural folds fuse midway along the neural groove, starting the formation of the neural tube (Nolte, 2009). By the end of the fourth week, additional sites of fusion appear, forming the entire neural tube (Nolte, 2009). The neural tube progressively separates from the ectodermal surface becoming enclosed within the body (Nolte, 2009). Cells from the crest of each neural fold develop into sensory neurons of the ganglia of spinal nerves, the postganglionic neurons of the autonomic nervous system (ANS), and the Schwann cells and satellite cells of the

PNS (Nolte, 2009). The neural tube develops into the CNS and its cavity develops into the ventricular system of the brain (Nolte, 2009).

During the fourth week, three bulges, referred to as the primary vesicles appear (Nolte, 2009; Figure I-2B). The most rostral is the prosencephalon, followed by the mesencephalon and finally the rhombencephalon. These vesicles merge smoothly with the spinal portion of the neural tube (Nolte, 2009). The prosencephalon develops into the cerebrum while the mesencephalon becomes the midbrain. The rhombencephalon develops into the rest of the brainstem and the cerebellum (Nolte, 2009). During the fifth week, the prosencephalon divides into the telencephalon and the diencephalon while the rhombencephalon divides into the metencephalon and the myelencephalon (Nolte, 2009). The telencephalon develops into the cerebral hemispheres (Nolte, 2009) and the diencephalon gives rise to the thalamus, the

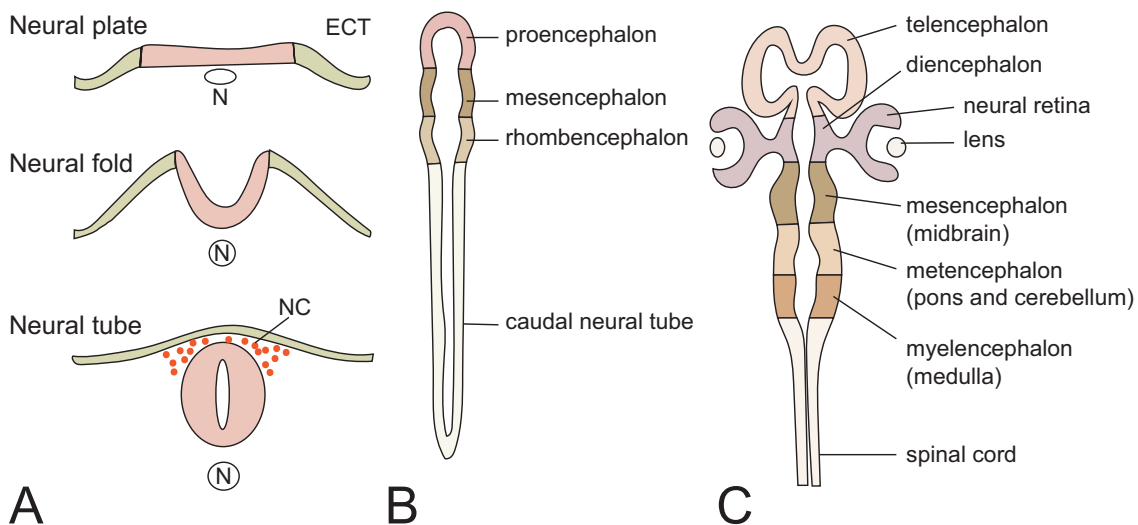


Figure I-2. Embryonic development of the vertebrate nervous system. A) The neural plate forms from the ectoderm (ECT), under which lies the notochord (N). During neurulation, the midline of the plate forms the neural fold. Fusion of the neural folds gives rise to the neural tube. Neural crest cells (NC) migrate from the dorsal region of the neural tube. **B)** Three primary vesicles develop that will give rise to the major structures of the brain. **C)** Secondary structures that develop from the primary vesicles.

hypothalamus, the retina, the optic nerve and several other structures (Nolte, 2009). The metencephalon becomes the pons and the cerebellum while the myelencephalon becomes the medulla (Nolte, 2009).

1.1.2 Central nervous system

The brain and spinal cord is made of white and gray matter (Purves *et al.*, 2001). Gray matter comprises of the neurons cell bodies and dendrites while white matter comprises of the axons (Purves *et al.*, 2001). The brain integrates, processes and coordinates the information it receives (Purves *et al.*, 2001). The spinal cord acts as a relay for motor and sensory information and coordinates certain reflexes. Motor information is transmitted from the brain down the spinal cord to the effector muscles while sensory information is relayed up the spinal cord to the brain. The glial cells of the CNS include astrocytes, oligodendrocytes, microglia and ependymal cells (Purves *et al.*, 2001). Astrocytes have star-like processes and are responsible for maintaining an appropriate chemical environment for neuronal signalling (Purves *et al.*, 2001). Oligodendrocytes are responsible for wrapping multiple axons with a lipid-rich sheath called myelin (Purves *et al.*, 2001). Myelin insulates the electrical signals as they travel down the axon, allowing for faster transmission of the signals (Purves *et al.*, 2001). Microglial cells are phagocyte-like cells that scavenge for cellular debris from injury or normal cell turnover (Purves *et al.*, 2001). Microglial cells can proliferate from resident microglia in the brain or migrate to a site and infiltrate the injured area from the blood stream (Purves *et al.*, 2001). Lastly, ependymal cells are the thin epithelial lining of the ventricles of the brain and the spinal cord (Purves *et al.*, 2001). These cells are responsible for the production of cerebrospinal fluid (CSF), which nourishes and protects the central nervous system from mechanical injury (Purves *et al.*, 2001).

The CNS is also protected by membranous coverings, called the meninges, which stabilize the position of the CNS (Nolte, 2009). The meninges are composed of three different layers. The outermost layer is the dura, followed by the arachnoid and the pia (Nolte, 2009). The dura is the thickest layer and is attached to the inner surface of the skull while the arachnoid adheres to the inner surface of the dura and the pia is attached to the brain. The space between the arachnoid and pia is filled with CSF and contains blood vessels (Nolte, 2009).

1.1.3 Peripheral nervous system

The PNS can be further divided into the ANS and the somatic nervous system (SNS) (Nolte, 2009). The ANS regulates processes in the body that are not consciously controlled, such as breathing and metabolic processes, while the SNS controls voluntary processes such as movement of the limbs (Nolte, 2009). Glial cells of the PNS include Schwann cells and satellite cells (Nolte, 2009). Unlike the oligodendrocytes, Schwann cells produce myelin around the axons of only a single neuron (Nolte, 2009). Schwann cells are also involved in regeneration and development of the neurons (Nolte, 2009). Satellite cells are similar to astrocytes in the CNS and play a role in regulating the environment in PNS ganglia (Nolte, 2009).

1.1.4 Regeneration of the nervous system

CNS axons do not readily regenerate after injury, whereas PNS axons do, allowing for recovery of function after peripheral nerve damage. Aguayo and colleagues have demonstrated that CNS neurons have the capacity to regenerate within the permissive environment of the PNS (Richardson *et al.*, 1980; David and Aguayo, 1981; Benfey and Aguayo, 1982). These studies suggested that neurons of the CNS are not intrinsically limited in their regenerative potential. Rather, the CNS has an inhibitory environment limiting the regenerative potential, whereas the

PNS has a stimulatory environment for axon regrowth. Indeed, growth promoting factors in the PNS and growth-inhibiting factors in the CNS have been implicated in axon regrowth. The upregulation of these factors is a consequence of the events that occur post-injury.

After injury to a peripheral nerve, the distal portion of the axon undergoes Wallerian degeneration (Figure I-3). This process leads to the disintegration of the axon. Within hours following injury, macrophages migrate to the site of injury to remove the debris (Faroni *et al.*, 2015). In the first 24 hours, Schwann cells proliferate and switch from a myelinating to regenerating phenotype, where upregulation of molecules to assist in the degenerative and regenerative processes occurs (Faroni *et al.*, 2015). Structural proteins, such as myelin basic protein and myelin associated glycoprotein are downregulated while cell adhesion molecules,

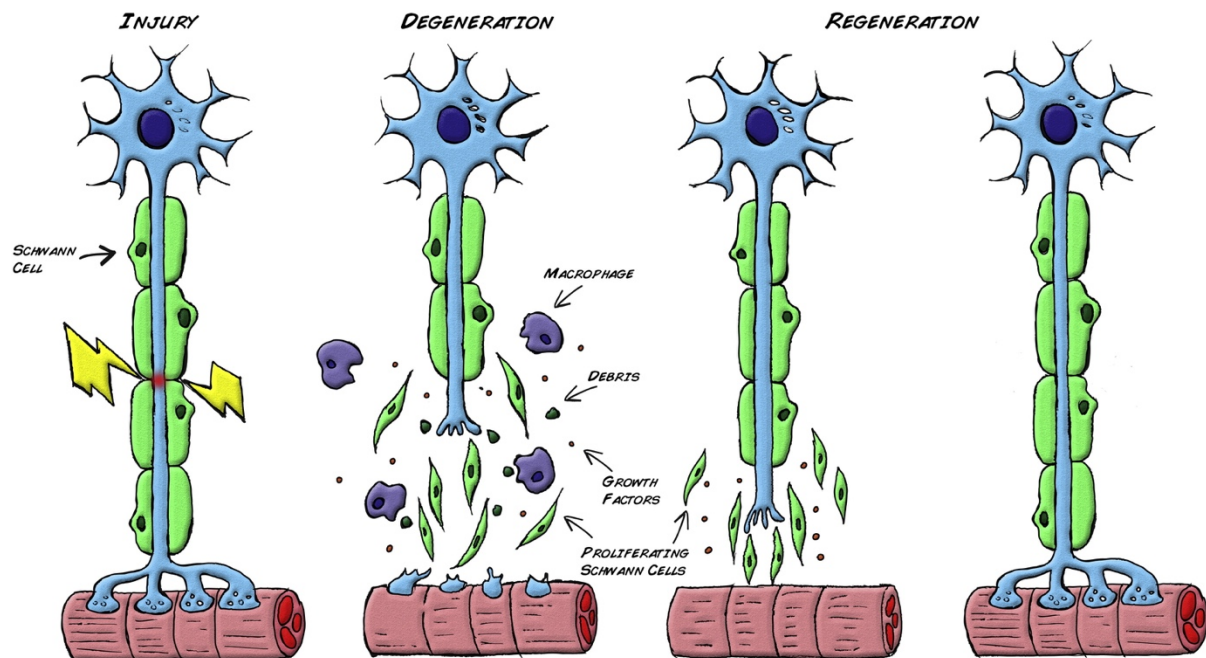


Figure I-3. Regenerative process in the PNS. Following injury and Wallerian degeneration, Schwann cells detach from axons and proliferate into a regenerative mode. In the regenerative mode, Schwann cells upregulate the expression of stimulatory factors, which creates a favorable environment for nerve regrowth and guidance. Figure reprinted from Faroni *et al.* (2015) with permission from Elsevier.

glial fibrillary acidic protein (GFAP) and growth factors – nerve growth factor (NGF), brain-derived growth factor (BDNF), glial-derived neurotrophic factor (GDNF), basic fibroblast growth factor (bFGF) and neurotrophin 3 (NT-3) are upregulated (Faroni *et al.*, 2015). Following removal of the debris, Schwann cells align into tubes called column bands of Bünger, which enable guided axonal regeneration in permissive environments that are rich in trophic factors (Faroni *et al.*, 2015).

After injury to CNS nerves, the distal ends of the axons form retracting dystrophic

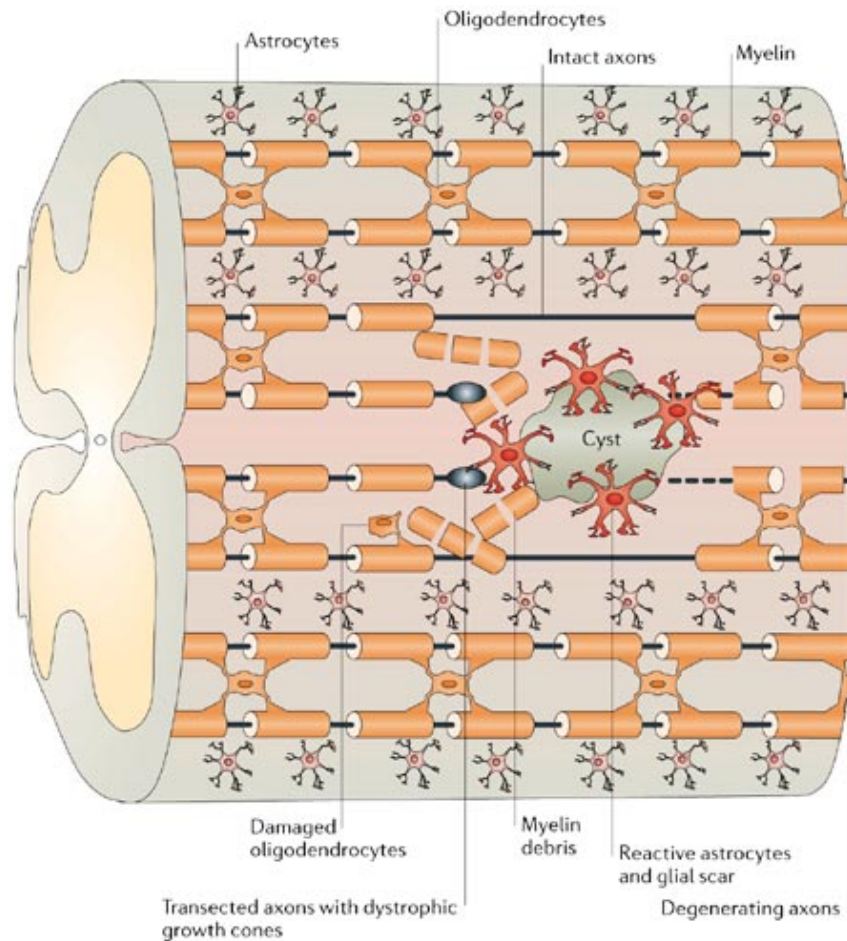


Figure I-4. Injury of axons in the CNS leads to the formation of a glial scar. MAIs and CSPGs create an inhibitory environment for axon regrowth. Figure reprinted from Yiu and He (2006) with permission from Nature Publishing Group.

growth cones (Yiu and He, 2006). During the early phase of injury, myelin associated inhibitors (MAIs) from intact oligodendrocytes restrict axon regrowth (Yiu and He, 2006). Next, recruitment of inflammatory cells and reactive astrocytes leads to the formation of a glial scar (Yiu and He, 2006; Figure I-4). The scar formation presents a physical barrier for regrowth and is also associated with an increased production of chondroitin sulphate proteoglycans (CSPGs), which further limits regeneration (Yiu and He, 2006).

Several of the myelin components expressed by the oligodendrocytes are MAIs. Mammalian CNS myelin predominantly consists of MBP and proteolipid protein (PLP) (Siegel *et al.*, 1999), with MBP comprising about 30% of the myelin sheath and PLP comprising another 40% (Siegel *et al.*, 1999). In contrast, the major PNS myelin protein is myelin protein zero (P₀) and accounts for more than half of the PNS myelin protein, while MBP in the PNS accounts for 5 to 18% of total protein (Siegel *et al.*, 1999). The remainder of the proteins in the CNS that make up the myelin sheath consists of other proteins and glycoproteins (Siegel *et al.*, 1999), some of which are MAIs. These proteins include Nogo-A, myelin-associated glycoprotein (MAG), myelin oligodendrocyte glycoprotein (MOG), ephrin-B3 and semaphoring 4D (Huebner and Strittmatter, 2009). Nogo-A, MAG and MOG interact directly with a neuronal Nogo-66 receptor (NgR1) which limits axon growth (Huebner and Strittmatter, 2009). Except for MAG, these MAIs are not produced by Schwann cells in the PNS (Huebner and Strittmatter, 2009). Still, MAG in the PNS is cleared away rapidly by glial cells in the periphery, unlike in the brain and spinal cord (Huebner and Strittmatter, 2009). Studies have demonstrated that removal of MAIs or blocking of the NgR1 receptor can promote regrowth in the CNS. Deletion of the Nogo-A gene in knockout mice has led to promotion of corticospinal tract growth and enhancement of functional recovery (Simonen *et al.*, 2003). Additionally, antibodies targeted

against Nogo-A promote axonal growth after CNS injury (Wiessner *et al.*, 2003). Although MAG has been shown to inhibit neurite outgrowth, no enhanced corticospinal tract regeneration was observed in MAG knockout mice (Bartsch *et al.*, 1995). Consequently, MAG may have less of an impact in limiting axon regrowth in the CNS compared to other MAIs. However, knockout of the NgR1 in mice led to differentially enhanced spinal tracts regrowth after spinal cord injury (Kim *et al.*, 2004). Moreover, regrowth of corticofugal axons was observed in these mice after a stroke (Li *et al.*, 2004). Thus, the method or location of injury in the CNS may be important factors for determining how MAIs will interfere with regeneration.

The astroglial scar, which forms as a result of reactive astrocytes, creates a physical barrier to regeneration and inhibits axon regrowth in the CNS (Yiu and He, 2006). The glial reaction to injury results in the recruitment of microglia, oligodendrocyte precursors, meningeal cells and astrocytes to the lesion site (Yiu and He, 2006). Many of the astrocytes become reactive, marked by an increase in GFAP, releasing CSPGs and other inhibitory extracellular matrix molecules (Yiu and He, 2006). CSPGs are the main inhibitory molecule found in the glial scar (Huebner and Strittmatter, 2009). They include neurocan, versican, brevican, phosphacan, aggrecan, and NG2 (Huebner and Strittmatter, 2009). A specific receptor for these molecules have not been identified (Huebner and Strittmatter, 2009). However, modifying the structure of CSPGs can promote regeneration. Specifically, CSPGs contain core proteins with glycosaminoglycan side chains, which, when cleaved by the bacterial enzyme chondroitinase ABC, reduces their inhibitory activity (Bradbury *et al.*, 2002).

Inflammation within the CNS also acts to inhibit the regenerative potential of axons. Microglial cells from the CNS and activated macrophages from the blood respond to trauma in the brain and spinal cord after injury (Fitch and Silver, 2008). These cells release their own

sources of cytokines and signaling molecules, leading to the upregulation of inhibitory molecules. The inflammatory response contributes to secondary damage after the primary insult (Fitch and Silver, 2008). Indeed, injection of an inflammation inducing agent in an *in vivo* model leads to significant axotomy and an upregulation of reactive astrocytes (Fitch and Silver, 2008). In contrast, some elements of CNS inflammation have been suggested to be neuroprotective. For example, macrophages can secrete growth promoting factors such as neurite growth factor and neurotrophin-3 (Elkabes *et al.*, 1996). Moreover, when zymosan is placed in the vitreous chamber of the eye, it can stimulate regeneration of optic nerve fibers (Leon *et al.*, 2000). Unfortunately, inflammation tends to create cavitation and scarring in the CNS in the absence of any primary physical injury (Fitch and Silver, 2008). It is unclear whether modifying immune cell activity could lead to functional regeneration within the CNS.

1.2 The eye and optic nerve

The vertebrate eye is an organ that allows an organism to detect light and process visual information. The human eye consists of several structures to help with this function (Figure I-5).

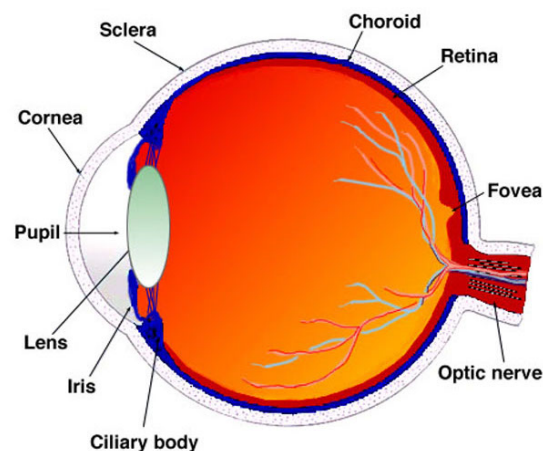


Figure I-5. Anatomy of the human eye. Figure reprinted from Kolb *et al.* (1995). with permission from <http://webvision.med.utah.edu/>.

A transparent layer of cells called the cornea acts to refract light entering the eye and cover the pupil and iris (Kolb *et al.*, 1995). The pupil allows light to enter the eye while the iris is a circular muscle that controls the size of the pupil, thus controlling the amount of light that enters the eye (Kolb *et al.*, 1995). Light is further and primarily refracted by the crystalline lens to produce a sharp image at the retina where the light is converted to an electrical signal by the neurons of the retina (Kolb *et al.*, 1995). This electrical signal is then sent to the brain via the optic nerve. The ciliary body and zonule fibers can also change the shape of the lens through a process known as accommodation, to focus the light onto the retina (Kolb *et al.*, 1995). The outermost layer of the human eye (Figure I-5), the sclera, is continuous with the cornea (Kolb *et al.*, 1995). The intermediate layer consists of the choroid and the innermost layer is the retina (Kolb *et al.*, 1995). The eye also consists of three chambers of fluid that provide nutrients to the various components of the eye. The anterior chamber, between the cornea and iris, and the poster chamber, between the iris, zonule fibers and lens is filled with aqueous humor (Kolb *et al.*, 1995). The aqueous humor maintains the intraocular pressure and inflates the globe of the eye (Kolb *et al.*, 1995). The vitreous chamber, between the lens and the retina, is filled with vitreous humor (Kolb *et al.*, 1995). The vitreous humor is an immobile gel-like substance that helps to hold the spherical shape of the eye and keep the retina in place (Kolb *et al.*, 1995).

1.2.1 Development of the eye and optic nerve

Development of the vertebrate eye begins in the primitive forebrain (Oyster, 1999). Two small bumps, referred to as optic pits, appear on either side of the neural tube as the rostral end closes (Oyster, 1999; Figure I-6). These pits form the beginning of the eyes and develop as a symmetric pair (Oyster, 1999). The pit undergoes cell proliferation to become a spherical vesicle connected to the neural tube by a cylindrical optic stalk (Oyster, 1999). Both the vesicle and

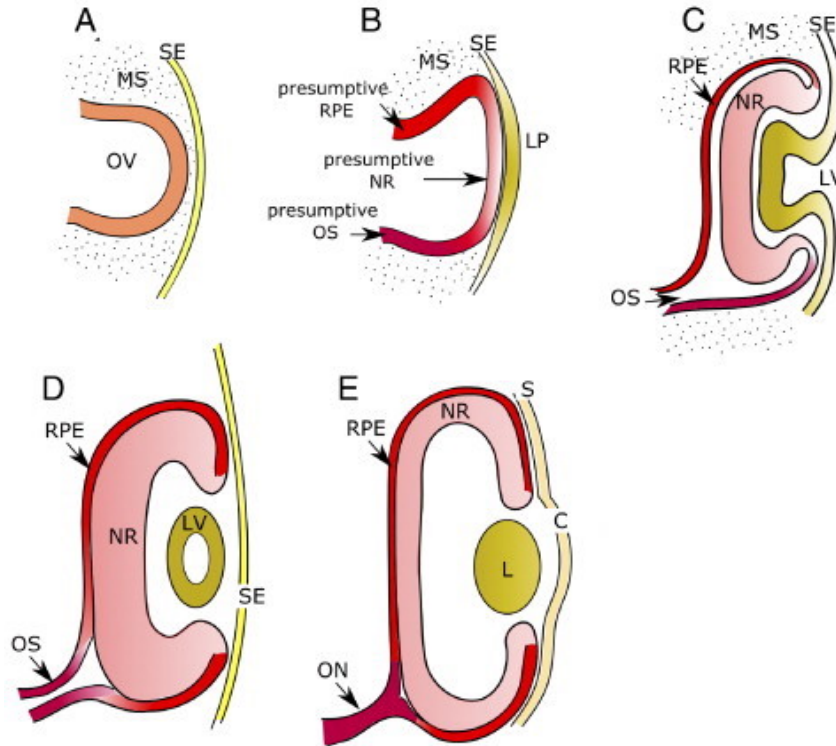


Figure I-6. Development of the vertebrate eye. A) An invagination from the diencephalon forms the optic vesicle. B) The optic vesicle contacts the surface ectoderm (SE) resulting in the formation of the future RPE, retina (NR) and optic stalk (OS) while the surface ectoderm forms the lens placode (LP). C) The optic stalk and lens placode invaginates to form the optic cup and lens vesicle (LV). D) The optic cup forms a bilayered hemisphere of the RPE and retina while the lens develops. E) The lens (L) becomes solid, and the optic stalk develops into the optic nerve (ON). The surface ectoderm gives rise to the corneal epithelium (C) and sclera (S). Figure adapted from Adler and Canto-Soler (2007) with permission from Elsevier.

stalk are hollow structures consisting of a layer of epithelial cells. These cells continue to expand but are limited by the surface ectoderm (Oyster, 1999). The optic vesicle then induces the surface ectoderm to form a lens (Oyster, 1999). As the lens forms, the optic cup invaginates more deeply to form the choroidal fissure (Oyster, 1999). The choroidal fissure appears along the inferior surface of the optic cup and stalk. With formation of the choroidal fissure, a blood vessel gains access into the optic stalk and extends to the rim of the cup and lens. This vessel begins as the hyaloid artery to supply the developing lens and portions of it eventually become the central retinal artery (Oyster, 1999). About 5-6 weeks into gestation, the choroidal fissure

closes and fusion of subsequent layers results in the optic cup assuming the form of a two-layered hemisphere (Oyster, 1999). At this point, the cells of the posterior part of the lens vesicle differentiate into lens fibers. These lens fibers will continue to develop to form the lens (Oyster, 1999). The outer rim of the cup will contribute to the iris, ciliary body and iris muscles, while the surface ectoderm will develop into the future corneal epithelium (Oyster, 1999). The mesoderm will eventually develop into the extraocular muscles, the orbit, and orbital vessels (Oyster, 1999). Meanwhile the optic cup and optic stalk represent the beginning of the retina and optic nerve, respectively (Oyster, 1999; Figure I-6).

The outer layer of the cup differentiates first, eventually producing the pigment epithelium in a center-to-periphery gradient (Oyster, 1999). Meanwhile, differentiation of the inner layer of the optic cup involves a thickening of a layer of stem cells and a migration of cells to eventually form the sensory retina (Oyster, 1999). These cells have the capacity to become any of the mature cell types in the retinas (Oyster, 1999). First retinal ganglion cells (RGCs), horizontal cells, and cones develop followed by amacrine cells, Müller cells, bipolar cells and rods (Oyster, 1999). Again, these cells develop in a center-to-periphery gradient, in the same order (Oyster, 1999). Synaptic connections develop a week after the first cells develop with the same gradient pattern (Oyster, 1999). Most of the neural connections within the retina are established by 5 months of gestation (Oyster, 1999). The synapses occur within two plexiform layers while the cell bodies of the retinal neurons are located in three nuclear layers (Figure I-7). The last structure to develop in the retina is the fovea. At the fovea, ganglion cell nuclei migrate radially outwards leaving an area of almost entirely developing cone cells, providing high visual acuity (Oyster, 1999). Foveal development continues until after about 4 years of birth (Oyster, 1999). After the initial wave of cells that develop in the central retina, vascular precursor cells

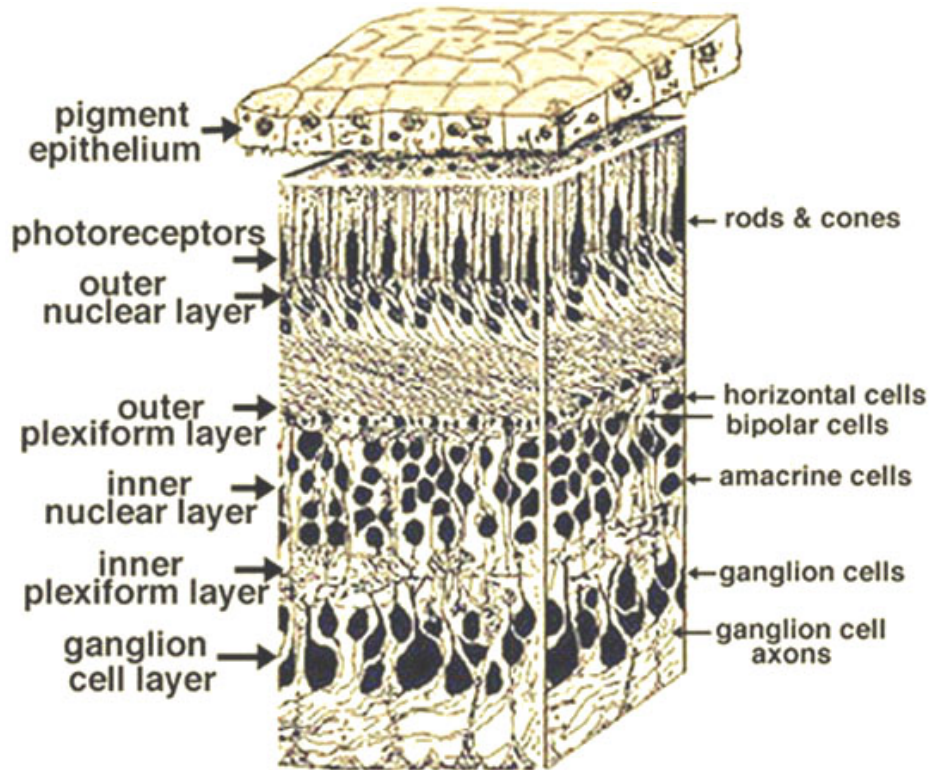


Figure I-7. 3-D block of a human retina. Photoreceptor nuclei are located in the outer nuclear layer (ONL) and synapse onto bipolar cells and horizontal cells in the outer plexiform layer (OPL). The nuclei of the bipolar, horizontal and amacrine cells are located in the inner nuclear layer (INL). Bipolar cells synapse with ganglion cells in the inner plexiform layer (IPL). However, amacrine and horizontal cells also influence the signals between the bipolar and ganglion cells. The ganglion cell nuclei are located in the ganglion cell layer (GCL) and their axons form the nerve fiber layer (NFL). Figure reprinted from Kolb *et al.* (1995) with permission from <http://webvision.med.utah.edu/>.

also appear eventually leading to the formation of blood vessels along the inner surface of the retina (Oyster, 1999).

The optic stalk is a hollow cylinder of neuroepithelial cells and folds inward to become a double-walled tube (Oyster, 1999). At this point, the stalk consists of three concentric parts: the central core and intermediate and outer sheaths of neuroepithelium (Oyster, 1999). The intermediate sheath will give rise to glial cells, including astrocytes and oligodendrocytes, within the nerve, while the outer sheath will become the outermost glial sheath of the nerve (Oyster,

1999). As axons from developing ganglion cells reach the nerve, the inner cells of the nerve core degenerate or differentiate into glial cells providing a path for the axons to the brain (Oyster, 1999). The optic nerve forms as the optic stalk is replaced by developing RGC axons and glial cells (Oyster, 1999). The growth of the dorsal part of the neural tube tends to push the stalks together eventually causing them to merge before arrival of the axons from the eyes. This fusion of the stalks produces the optic chiasm (Oyster, 1999). The retinotopic distribution of axons in the nerve and chiasm is retained and provides directions for the ipsilateral or contralateral path (Oyster, 1999). Finally, at about fetal week 15, oligodendrocytes in the nerve begin to form myelin sheaths around the axons in a center-to-periphery gradient reaching the lamina cribrosa before birth where myelination stops (Oyster, 1999). About 90% of the tract axons will project to the lateral geniculate nucleus (LGN) on either side of the midbrain as part of the primary visual pathway (Oyster, 1999). Meanwhile, the other 10% of the ganglion cell axons will terminate in other regions of the brain such as the superior colliculus, the pretectal nuclei, and the suprachiasmatic nucleus for other functional associations (Oyster, 1999).

1.2.2 Diseases of the optic nerve

The optic nerve is part of the CNS. Consequently, like the brain and spinal cord, the optic nerve does not readily regenerate after injury. Injury to the optic nerve typically results in permanent loss of axons and RGCs. Consequently, loss of the RGCs results in vision loss or blindness depending on the severity of the damage. The most common diseases to affect the optic nerve are glaucoma, inflammatory optic neuritis and ischemic optic neuropathy (Margalit and Sadda, 2003).

Glaucoma is a disease characterized by the progressive degeneration of RGCs, cupping of the optic nerve, and visual loss (review by Weinreb *et al.*, 2014). Glaucoma is currently the

leading cause of irreversible blindness worldwide, affecting more than 70 million people (Weinreb *et al.*, 2014). The biological basis of the disease remains poorly understood, and affected individuals could be asymptomatic until signs of damage become apparent (Weinreb *et al.*, 2014). There are several types of glaucoma, however the most common, open-angle glaucoma, represents more than 80% of the cases observed (Weinreb *et al.*, 2014). Currently, intraocular pressure is the most important risk factor associated with glaucoma (Weinreb *et al.*, 2014). An increase in intraocular pressure, due to an imbalance of aqueous humor production and secretion, results in mechanical stress and strain on the structures of the back of the eye, namely the lamina cribrosa (Weinreb *et al.*, 2014). The lamina cribrosa is where the sclera passes through the axons of the RGCs in a mesh-like fashion. It presents the weakest point in the wall of the eye. Consequently, pressure-induced strain, compression, deformation or remodelling of the axons can all result in mechanical damage to the axons and disrupt axonal transport and ultimately result in the degeneration of RGCs via apoptosis (Weinreb *et al.*, 2014).

Optic neuritis is a demyelinating inflammation of the optic nerve. There are several clinical classifications of optic neuritis (review by Toosy *et al.*, 2014). However, it is most commonly associated with multiple sclerosis (MS), an autoimmune disease of the CNS that targets myelin and results in inflammation and vision loss (Toosy *et al.*, 2014). The pathology presents itself as lesions in the optic nerve, similar to plaque formation in the brains of MS patients (Toosy *et al.*, 2014). In the early phase of the disease, inflammatory demyelination occurs, resulting in conduction block and visual loss (Toosy *et al.*, 2014). T-cell, B-cell and microglial activation occurs with a release of pro-inflammatory cytokines (Toosy *et al.*, 2014). However, the specific mechanism and target antigens are unknown. Several weeks following an acute episode, inflammation resolves and visual function and remyelination are incompletely

restored (Toosy *et al.*, 2014). Additionally, damaged axons become more vulnerable to future inflammatory episodes (Toosy *et al.*, 2014). While a high dose of intravenous corticosteroids could speed the recovery of visual function, it does not have an effect on the ultimate visual outcome (Margalit and Sadda, 2003).

Unlike optic neuritis which is due to inflammation, ischemic optic neuropathy (ION) is due to ischemia. ION is the most common form of optic neuropathy in older patients (review by Biousse and Newman, 2015). ION can be classified as anterior- or posterior-ION based on the segment of the optic nerve affected, although 90% of cases present as anterior ION. Anterior- and posterior-ION can be further classified as nonarteritic or arteritic (Biousse and Newman, 2015). Nonarteritic anterior ION results from disease of the small vessels supplying the anterior segment of the optic nerve, however the exact cause is unknown. Hypoperfusion of the posterior ciliary artery branches leads to optic nerve ischemia and compression of the axons and capillaries in the optic nerve head ultimately leading to axonal loss and subsequent vision loss (Biousse and Newman, 2015). There are currently no established treatments for nonarteritic anterior ION (Biousse and Newman, 2015). Arteritic ION is caused by inflammation of the arteries (arteritis), particularly the cranial branches of the aortic arch including the ophthalmic and ciliary arteries. Again, the precise mechanism of the disease is unknown and may be determined by a wide variety of factors such as genetics, autoimmunity and environment (Biousse and Newman, 2015). If the arteritis is left untreated, transient visual loss caused by optic nerve or choroidal ischemia precedes permanent visual loss by days to weeks (Biousse and Newman, 2015). Immediate treatment is possible with the use of glucocorticosteroids to prevent further visual loss in the unaffected eye but does not reverse the existing visual loss (Biousse and Newman, 2015).

1.2.3 Optic nerve regeneration

Studies have focused on regenerating RGCs by targeting the same factors that prevent regeneration in other CNS tissues. These factors include: preventing neuronal (RGC) cell death, activating the RGC growth state and counteracting inhibitory signals in the extracellular environment. As in the brain and spinal cord, MAIs such as Nogo-A, MAG, and MOG suppress optic nerve axon growth. Additionally, CSPGs that accumulate in the glial scar at the site of injury also inhibit axon growth. Overcoming these factors can help to regenerate the optic nerve.

The use of trophic factors can help provide a source of neuroprotection. The classical neurotrophins, namely BDNF, and neurotrophin 4/5 (NT-4/5) bind to tyrosine kinase receptors expressed on RGCs (Fischer and Leibinger, 2012). Both of these molecules mediate proliferation, differentiation, axon growth and dendrite and synapse formation in the CNS (Ebadi *et al.*, 1997). Additionally, cytokines of the IL-6 family, namely leukemia inhibitory factor (LIF) and ciliary neurotrophic factor (CNTF) have also been shown to be neuroprotective (Leibinger *et al.*, 2009). Both of these cytokines involve the signal transducing receptors glycoprotein 130 and LIF receptor, which are both expressed by RGCs (Fischer and Leibinger, 2012). Other growth factors such as fibroblast growth factor (FGF), GDNF, hepatocyte growth factor (HGF) and granulocyte-macrophage colony stimulating factor (GM-CSF) also increase the survival of RGCs after optic nerve injury (Fischer and Leibinger, 2012). It remains unclear whether these growth factors have a direct effect on the RGCs or if the effects are a consequence of activating other retinal cells. For example, intravitreal injection of CNTF activates retinal glia to express and release endogenous CNTF (Muller *et al.*, 2009). BDNF has been shown to be the most effective survival agent for axotomized RGCs, however the effects of BDNF and other factors are transient and only delay the progress of neuronal degeneration, as the injured axons do not

regrow (Di Polo *et al.*, 1998). Consequently, neuroprotection itself cannot be sufficient for complete regeneration of RGCs.

Benowitz' group discovered that puncture of the ocular lens induces a robust regenerative response in axotomized RGCs (Leon *et al.*, 2000). Lens injury also enables RGCs to regenerate axons into the inhibitory environment of a crushed optic nerve (Leon *et al.*, 2000; Yin *et al.*, 2003). This result indicates a neuroprotective, growth promoting and disinhibitory effect on RGCs, because of lens injury. The beneficial effects of the lens injury, termed inflammatory stimulation (IS), were attributable to the activation of retinal astrocytes/Müller cells and infiltrated macrophages (Muller *et al.*, 2007; Leibinger *et al.*, 2009). IS induces the constant expression of neuroprotective CNTF and LIF in retinal astrocytes allowing for significantly greater neuroprotection and regeneration than compared to intravitreal administration (Muller *et al.*, 2007; Leibinger *et al.*, 2009). Indeed, viral expression of constant CNTF allowed axons to reach the optic chiasm 5 weeks after an intraorbital nerve crush (Leaver *et al.*, 2006). Additional glial or macrophage-derived factors may synergistically contribute to this regeneration (Yin *et al.*, 2003).

RGC axons are capable of growing into a peripheral nerve graft transplanted into the stump after transection (Aguayo *et al.*, 1987; Vidal-Sanz *et al.*, 1987). These axons were able to grow back to and form synapses in the superior colliculi (Vidal-Sanz *et al.*, 1987). These studies indicated the inhibitory environments role in suppressing optic nerve axon growth. Knockdown of Nogo receptors (NgR), the receptor family to which all three major MAIs can bind, markedly enhanced regeneration in the optic nerve *in vivo* when RGCs were also activated by lens injury, while knockdown of NgR alone showed almost no improvement in axonal regeneration (Fischer *et al.*, 2004; Su *et al.*, 2009). CSPGs from the glial scar presents another source of inhibition for

optic nerve regeneration. Knockout of a recently hypothesized receptor for CSPGs in mice demonstrated reduced sensitivity in culture and enhanced axonal regeneration beyond the scar in the optic nerve (Sapieha *et al.*, 2005). Thus, overcoming the inhibitory environment after injury can help to enhance axonal regeneration.

1.3 The chick model

1.3.1 Anatomical differences of the chick retina and optic nerve

Development of the chick retina is like other vertebrates such as humans and rats. Invagination of the optic vesicle leads to the formation of two layers. The retina is derived from the thickened inner layer while the outer layer will form the sclera, choroid and retinal pigment epithelium (Mey and Thanos, 2000). Retinal development is essentially completed at the time of hatching (Mey and Thanos, 2000). The first cells to differentiate, in a center-to-periphery gradient are the RGCs, followed by the photoreceptors, amacrine cells, horizontal cells and bipolar cells (Mey and Thanos, 2000). This sequence occurs in a stereotypic order but with overlap (Mey and Thanos, 2000). This order differs from that of humans which occurs in two groups: retinal ganglion cells (RGCs), horizontal cells, and cones followed by amacrine, Müller, bipolar cells and rods (Oyster, 1999). Like the fovea in human, the chick also has a region specialized for high visual acuity called the area centralis (Mey and Thanos, 2000). This area extends from the central retina, temporal to the dorsal edge of the pecten, to the superior temporal quadrant as a streak (Mey and Thanos, 2000).

Unlike humans and other vertebrates, oligodendrocyte precursors are observed in the inner retina around E14 (Nakazawa *et al.*, 1993). These cells migrate from the optic nerve into the retina and spread through the nerve fiber layer (Nakazawa *et al.*, 1993). Oligodendrocyte

differentiation starts during the third embryonic week and increases one week after hatching (Nakazawa *et al.*, 1993). Most of the myelination of the axons takes place during the early postnatal period (Mey and Thanos, 2000)

In contrast to other vertebrates, the avian retina is devoid of blood vessels but contains the pecten, a vascularised organ which projects from the optic disc into the vitreous body (Mey and Thanos, 2000). The vessels supplying the pecten run lateral of the optic nerve head and consist of several arterial and venous branches (Uehara *et al.*, 1990). Subsequently, macrophages migrate from the pecten into the periphery of the retina. However, in humans and rats, these cells invade the retina from the peripheral margins via the blood vessels of the ciliary body and from the future central retinal artery, which passes through the optic nerve (May, 2008).

1.3.2 Optic nerve damage studies in chicks

The majority of optic nerve damage studies on the chicken model have focused on regenerating retinal neurons. Following excitotoxic injury to the retina, Müller glia in the retina can serve as a source of retinal progenitors. However, this source is only available for the first few days post-hatch (Fischer and Reh, 2001). Moreover, Müller glia-derived cells in the retina either do not survive or fail to differentiate (Fischer and Reh, 2001). RGC-dependent optic nerve regeneration is limited in the chick. Retinae from chick embryos are able to regenerate but this ability declines rapidly post-hatch (Goldman and Hyde, 2014). Fischer and colleagues (2002) induced damage to RGCs via kainate-induced excitotoxicity and colchicine injections, which selectively destroy ganglion cells. They observed some regeneration of colchicine- and kainate-treated ganglion cells after intravitreal injections of growth factors insulin and FGF-2 (Fischer and Reh, 2002). Glucocorticoid signalling is also known to suppress inflammation and microglial and

macrophage reactivity (Gallina *et al.*, 2015). The receptors for glucocorticoid (GCR) are known to be localized to the nuclei of Müller glia (Gallina *et al.*, 2015). Fischer's group also demonstrated that activation of GCRs promoted the survival of colchicine-damaged ganglion cells and excitotoxin-damaged amacrine and bipolar cells, and photoreceptors in detached retinas (Gallina *et al.*, 2015). The survival-promoting effects were attributable to the suppression of microglial activity as a result of the GCR activation in Müller glia (Gallina *et al.*, 2015).

1.4 Kynurenic acid

Kynurenic acid (KYNA) is a substance that is normally found in the body in astrocytes of the brain (Guillemin *et al.*, 2001). It has activity in regulating normal physiological processes and has both toxic and protective effects. However, KYNA is only one of the neuroactive metabolites derived from tryptophan. Collectively, these neuroactive intermediates, termed “kynurenines,” have been linked to neurophysiological processes and several brain diseases. Illuminating the toxic or neuroprotective effects of these compounds can help to better understand the mechanisms responsible for CNS damage and regeneration.

1.4.1 The kynurenine metabolic pathway

Dietary tryptophan is metabolized via the kynurenine pathway which is initiated by the oxidative opening of the indole ring and eventually produces nicotinamide adenine dinucleotide (NAD⁺) (Schwarcz and Pellicciari, 2002). L-kynurenine (L-KYN) is the major primary degradation product of tryptophan which subsequently leads to three neuroactive compounds. L-KYN is converted to KYNA in a dead-end side-arm pathway. L-KYN is also converted to 3-hydroxykynurenine (3-HK) which is then converted to quinolinic acid (QUIN) eventually leading to NAD⁺ formation (Schwarcz and Pellicciari, 2002; Figure I-8).

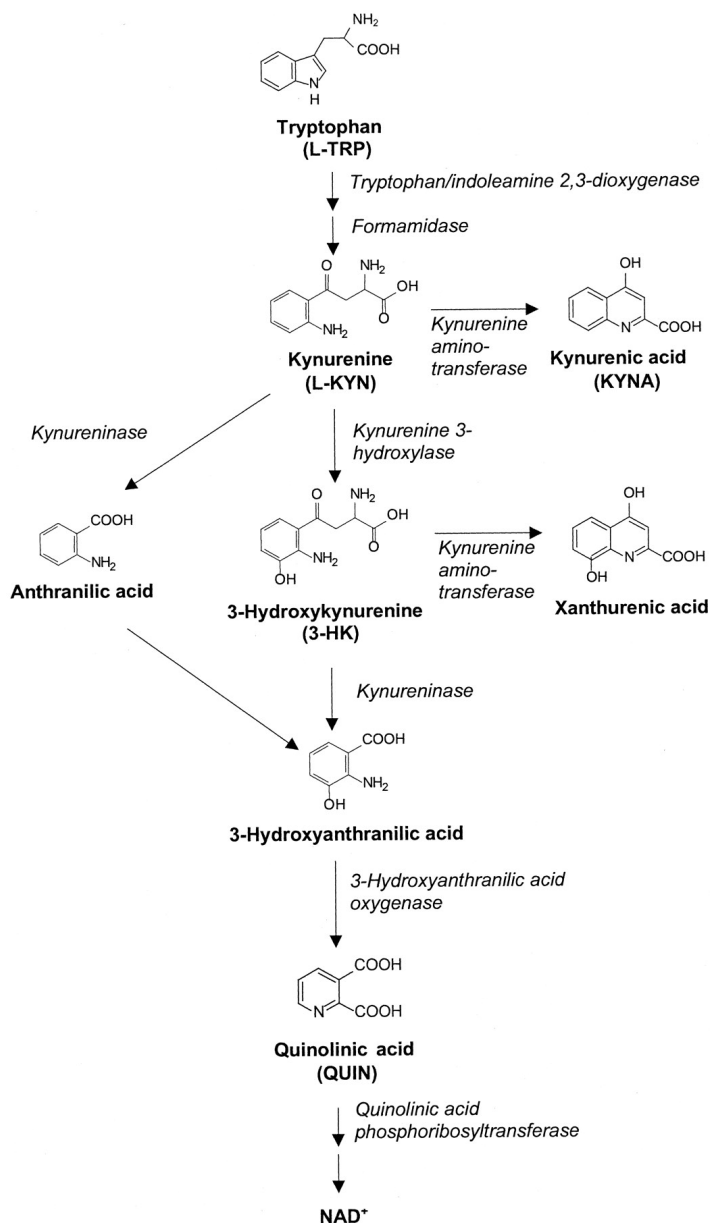


Figure I-8. Kynurenine metabolic pathway. Tryptophan is metabolized to L-KYN which is then converted to KYNA in a dead-end side arm pathway. L-KYN also leads to the production of QUIN and ultimately NAD⁺. Figure reprinted from Schwarcz *et al.* (2002) with permission from the Journal of Pharmacology and Experimental Therapeutics.

Kynurenine aminotransferases (KATs) catalyze the irreversible transamination of L-KYN to KYNA and metabolizes 3-HK to xanthurenic acid, an inert side product. 3-HK is also converted to 3-hydroxyanthranilic acid (3-HANA) by kynureninase. 3-Hydroxyanthranilic acid

oxygenase (3-HANA O) then converts 3-HANA to a product which rearranges non-enzymatically to form QUIN. L-KYN and 3-HK can be produced by the brain but primarily enters from blood circulation via neutral amino acid transporters and are then taken up by astrocytes and microglial cells (Fukui *et al.*, 1991). There are two forms of KATs in the brain (KAT I and KAT II). Both forms have a high affinity for L-KYN in the low millimolar range but differ in their optimum pH range and substrate specificity. KAT I has a pH optimum of 9.5 to 10 with little substrate specificity, whereas KAT II operates best at physiological pH and preferentially recognizes L-KYN as a substrate (Guidetti *et al.*, 1997). The enzymes to produce brain kynurenines are localized to astrocytes and microglial cells. Astrocytes lack kynurenine 3-hydroxylase thus favouring KYNA production, whereas microglial cells preferentially form QUIN due to limited KAT activity (Guillemin *et al.*, 2001). The cell specific separation creates a dichotomy between the two metabolic arms of the pathway.

1.4.2 Kynurenines in neurological diseases

Huntington's disease is an adult-onset neurodegenerative disorder caused by the expansion of a CAG repeat in the gene encoding *huntingtin*. Huntington's disease presents the most amount of evidence for a pathological role of abnormal levels of kynurenines. QUIN was found to be significantly elevated to excitotoxic levels in post-mortem brains, coinciding with activation of microglia (Whetsell and Schwarcz, 1989). The increase in QUIN was also associated with elevated levels of 3-HK (Guidetti *et al.*, 2004). Indeed, the elevation of both microglia-derived kynurenines present a synergistic neurotoxic effect (Guidetti and Schwarcz, 1999). A reduction of KYNA levels also appears to enhance vulnerability to QUIN neurotoxicity (Sapko *et al.*, 2006).

Parkinson's disease is a chronic neurodegenerative disorder characterized by the loss of dopaminergic neurons and the presence of protein aggregates (Zinger *et al.*, 2011). In Parkinson's disease, the concentration of 3-HK is increased while kynurenine and KYNA levels are slightly reduced (Ogawa *et al.*, 1992). Moreover, QUIN levels significantly exceed KYNA levels, resulting in the degeneration of dopaminergic neurons in the substantia nigra of Parkinson's disease patients (Tan *et al.*, 2012).

Alzheimer's disease is a progressive neurological disorder characterized by impaired brain function due to the formation of amyloid plaques, neurofibrillary tangles, and gliosis. In Alzheimer's disease, QUIN excitotoxicity seems to be strongly associated with amyloid plaque formation (Guillemin *et al.*, 2005).

Ketamine, a drug which induces schizophrenia-like symptoms in normal individuals, and exacerbates psychotic features in patients with schizophrenia, functions as an NMDA receptor antagonist, like KYNA (Anis *et al.*, 1983). Indeed, KYNA levels are elevated in post-mortem brains of patients with schizophrenia, while 3-HK levels are unchanged (Erhardt *et al.*, 2001; Schwarcz *et al.*, 2001). As expected, elevation of KYNA leads to a greater inhibition of $\alpha 7$ nAChRs which results in an imbalance of glutamate, dopamine and acetylcholine systems in the brain and have all been linked to schizophrenia pathology (Erhardt and Engberg, 2002).

Neuroinflammation plays a significant role in the pathogenesis of many neurological diseases. After damage or trauma to the CNS, circulating immune cells infiltrate the brain, resident microglia are activated and an influx of blood derived, pro-inflammatory cytokines and other immune factors occurs. These mechanisms enhance the synthesis of kynurenine from tryptophan within the brain (Saito *et al.*, 1992; Saito *et al.*, 1993). However, the various cytokines have distinct roles on the activity of the enzymes involved in the production of

kynurenines. After systemic lipopolysaccharide administration in rat brains, which induces inflammation, pro-inflammatory mediators increased the expression of kynurenine-3-monooxygenase leading to increased levels of 3-HK and QUIN, while KAT II expression was unaffected (no change in KYNA levels)(Connor *et al.*, 2008). MS, is a demyelinating autoimmune disease of the CNS characterized by the presence of peripheral immune cells within sites of active demyelination (Carson, 2002). In MS patients experiencing remission, KYNA levels in CSF are significantly decreased. However, in MS patients undergoing acute clinical exacerbation, KYNA levels are elevated in CSF and plasma (Rejdak *et al.*, 2002; Rejdak *et al.*, 2007). Thus, it's believed that the changes in KYNA concentrations are a result of compensatory mechanisms to neurotoxicity.

1.5 Drug delivery to the optic nerve

Conventional methods of drug delivery to the eye include topical drops and intravitreal injections however novel drug delivery systems using nanoparticles and implants are currently being developed (Patel *et al.*, 2013). Topical eye drops are the most preferred and least invasive method of drug administration however the physiological and anatomical barriers of the eye make this a poor method of delivery to the posterior segment. Due to rapid draining through the nasolacrimal ducts, low permeability of the corneal epithelium, systemic absorption and the blood-aqueous barrier less than 5% of a drug will reach deeper ocular tissues, making it difficult to achieve therapeutic drug concentrations at the posterior tissues (Patel *et al.*, 2013). Intravitreal injections are the most commonly used route of drug administration to treat posterior segment diseases. However, like topical eye drops, this method does not provide a sustained delivery system. The use of repeated intravitreal injections, to mimic a sustained delivery system, may also lead to endophthalmitis, hemorrhages and retinal detachment (Patel *et al.*, 2013).

Nanoparticles are colloidal carriers that have a size range of 10 to 1000 nm (Patel *et al.*, 2013). They are generally composed of lipids, proteins or natural or synthetic polymers such as polylactic acid (Patel *et al.*, 2013). Drugs can be enclosed within the polymeric shell of the particle and can demonstrate sustained release (Patel *et al.*, 2013). Following periocular administration in Sprague Dawley rats, 200 – 2000 nm sized particles were retained at the site of administration for two months (Amrite and Kompella, 2005). More recently, trans-meningeal drug delivery to the optic nerve has been demonstrated using a nanoparticle delivery system with a controlled, sustained, release of brimonidine (Grove *et al.*, 2014). However, this method requires that the compound pass through the selectively permeable dural sheath and has only been demonstrated *in vitro*. Nanoparticle development and testing would also be required to confirm delivery and flow rates of the compound. An injection would still be required to ensure local delivery of the nanoparticles.

Intraocular implants are specifically used to provide localized and sustained drug release over a set duration. For posterior segment tissues, implants are typically placed intravitreally by making an incision at the pars plana, allowing for the delivery system to bypass the blood retinal barrier (Patel *et al.*, 2013). However, this type of delivery system is still limited to delivering compounds from the vitreal chamber, making it difficult to ensure that an adequate dose spreads the full length of the optic nerve. Alzet osmotic pump implants have been used by several groups to deliver agents directly to the optic nerve at constant flow rates (Hodges-Savola *et al.*, 1996; Rogers, 2003; Chauhan *et al.*, 2004; Aktas *et al.*, 2010). However, these devices require a much more invasive means of targeting the tissue. Aktas *et al* (2010), placed the catheters from the mini-pumps in the anterior portion of the optic nerve from a surgically created sub-Tenon space in rabbits. In rats, Chauhan *et al* (2004) exposed the optic nerve by blunt dissection through an

incision over the orbital ridge. A small hole in the orbital ridge was made by drilling through it. Then the catheter was fed through and held in place by gluing it to the ridge while leaving the end of the catheter just above the nerve. Hodges-Savola (1996) and Rogers (2003) both dissected the superior extraocular muscles to expose the optic nerve in rabbits. The catheter was then placed under the dural sheath of the nerve. However, removal of the extraocular muscles may have significant effects on the growth and development of the eye (Greene, 1981; Zhou *et al.*, 2011).

II: INTRODUCTION

The CNS, unlike the peripheral nervous system, does not readily regenerate after damage. The inability to successfully regenerate is thought to occur due to a non-permissive cellular environment following damage to the structures; inhibitory molecules, such as myelin produced by glial cells and inflammatory molecules, lead to the formation of a glial scar and permanent damage (Weibel, 1994; Hernandez, 2000).

A study by Dabrowski and colleagues (2015) revealed that prolonged infusion of a high dose of kynurenic acid (KYNA) could effectively reduce the myelin content in the spinal cord without severe damage to the glial cells or an inflammatory cascade, illuminating a potential role for KYNA to act as an inhibitor of myelin production. KYNA has also been shown to elicit neuroprotective effects after central nervous system (CNS) injury (Hsieh *et al.*, 2011; Zadori *et al.*, 2011; Korimova *et al.*, 2012) indicating that changes to KYNA concentrations and prolonged vs single dose administration of KYNA can have markedly different effects on the neurophysiology of the brain and spinal cord. Thus, it is reasonable to suspect that KYNA may be a useful mediator of myelin proteins during optic nerve damage, which may help to provide a more permissive environment for the regenerative process. The purpose of the following study was to determine the effects of KYNA on the myelination of the chicken optic nerve.

III: MATERIAL AND METHODS

3.1 Animals

All procedures in this study were conducted in accordance with the Guidelines of the Canadian Council on Animal Care. All protocols were approved by the University of Waterloo Animal Care Committee. A total of 31 mixed, unsexed White Leghorn hatchlings (*Gallus gallus domesticus*) were obtained from Maple Leaf Poultry in New Hamburg, Ontario and were fed ad libitum. Chicks were housed in stainless steel brooders with a heat source and kept on a 12 h: 12 h light-dark cycle. The chicks were randomly assigned to one of three treatment groups. Chick optic nerves were unilaterally infused with either KYNA (group I), PBS (group II), or received no treatment (group III). Chicks that received no treatment served as negative controls (NC).

3.2 Implantation

At 7 days old, chicks were induced and maintained with 2-2.5% isoflurane in oxygen. Seven day old chicks were selected to provide the optimal conditions necessary for the success of the implantation. The skin near the left eye, head, and neck were shaved and disinfected. An incision was made at the lateral canthus of the left eye (treated). The optic nerve of the left eye was exposed by spreading the lateral rectus and superior rectus muscles apart. The dura was cut and superficially spread apart. A rat intrathecal catheter (0007741, Alzet, Durect Corporation, Cupertino, CA) was then placed between the extraocular muscles and into the nerve, under the dural sheath (Figure III-1).

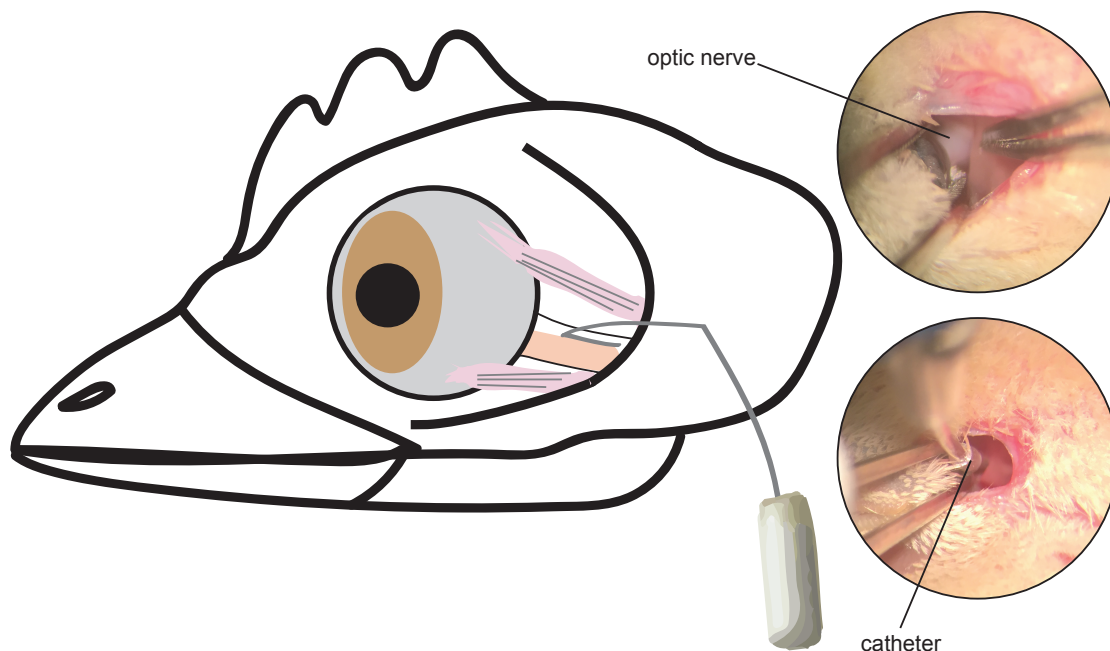


Figure III-1. Illustration describing the surgical procedure with images indicating exposure of the optic nerve and catheter insertion. Optic nerves were exposed by carefully spreading apart the extra ocular muscles. The catheter was then inserted under the dural sheath and fixed to the tissue with a drop of tissue glue.

A drop of Vetbond Tissue Glue (10872, CDMV, St-Hyacinthe, Quebec) was added to hold the catheter in place. The catheter was also held in place with a suture to the fascia at the lateral canthus. The remaining external portion of the catheter was placed under the skin toward the back of the head where it was connected to an osmotic pump (Model 1007D, Alzet, Durect Corporation, Cupertino, CA). The pumps were pre-loaded with either KYNA (K3375, Sigma-Aldrich, Oakville, Ontario) or PBS. 0.473 g of KYNA was diluted in 50 mL of PBS and slowly titrated with 1 normal NaOH to raise the pH to 7.5. Diluted KYNA or PBS was filter-sterilized with a 0.2 micron syringe-top milliQ filter before being injected into the osmotic pumps. The pumps were then placed subcutaneously in the lower back neck region. The skin at the lateral canthus and back of the head were sutured using ophthalmic silk braided 7-0 G-6 sutures (104965, CDMV, St-Hyacinthe, Quebec). After the surgery, chicks received a 0.1 mL injection

of a 1:10 diluted solution of meloxicam (Metacam 0.5%, 104674, CDMV, St-Hyacinthe, Quebec) subcutaneously for postoperative analgesia and polysporine was generously spread over the incision and implantation sites. The right eye (control) of the birds that underwent surgery was left untouched. Chicks received subdural infusion of either KYNA or PBS, at a flow rate of 0.5 μ l/hr, for seven days into the left optic nerve. All chicks were monitored daily for signs of complications and general health.

KYNA-infused, PBS-infused, and birds that received no treatment were euthanized with an intraperitoneal injection of 75 mg/kg body weight sodium pentobarbital (McGill University, Quebec) and the chest was opened. A dose of 100 IU heparin (105763, CDMV, St-Hyacinthe, Quebec) was injected into the left ventricle prior to cardiac perfusion with lactated Ringer's solution (4395, CDMV, St-Hyacinthe, Quebec). For histology and electron microscopy birds were perfused with Karnowski's fixative following the lactated Ringer's solution.

3.2.1 Validation of the implantation technique

A subset of chicks was used to validate the surgical procedure by infusing the nerves with India ink. Chicks that were infused with India ink into the left nerve show a clear color change due to the infiltration of the black dye (Figure III-2). The dye was present throughout the optic chiasm and the contralateral nerve. In contrast, the negative control and PBS-infused birds did not show any colour change (Figure III-2).

3.3 Histology and electron microscopy

The tissues of the brain and optic nerve of KYNA-infused (n = 7), PBS-infused (n = 3) and negative controls (n = 4) chicks were removed carefully and post fixed in Karnowski's. During the dissection, nerves were inspected to confirm the location of the catheter within the nerve.

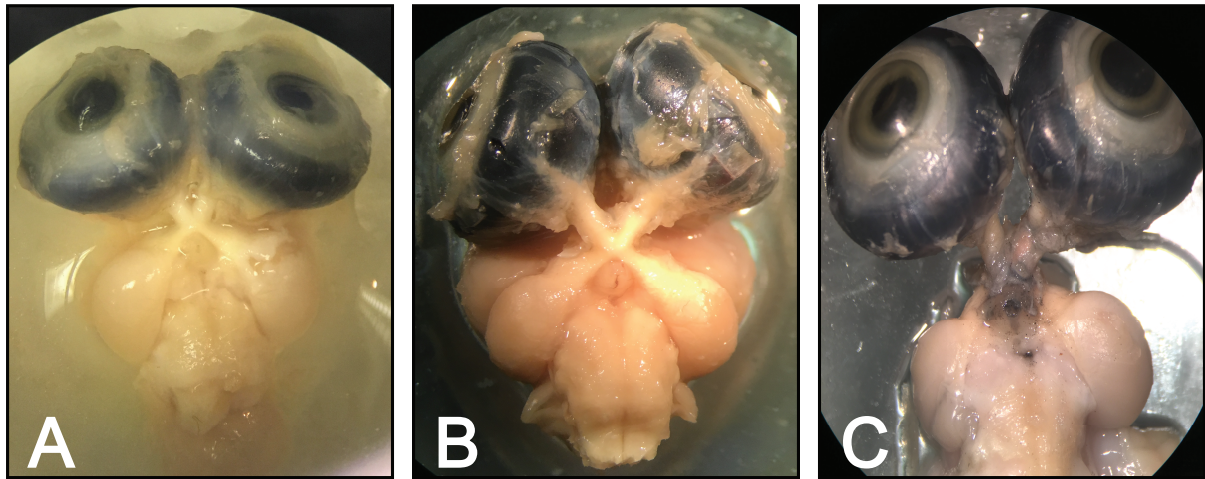


Figure III-2. Validation of the implant procedure. Dissected Negative control (A), PBS-infused (B), and India Ink-infused (C) optic pathways and brain matter. India Ink-infused birds show a clear colour change due to the infusion of black dye under the dural sheath.

Optic nerves were cut and submitted to the HSC Electron Microscopy Facility at McMaster University for embedding in epon/aradite resin. For histology, 1 μm thick sections, from the optic nerve head, were cut with a glass knife, mounted on a glass slide and stained with toluidine blue. These sections were analyzed under a Nikon Eclipse 50i microscope. Silver gray ultrathin sections from epon-embedded portions of the nerve were mounted on Formvar coated copper grids, stained with uranyl acetate and lead citrate and examined under a Jeol 1200EX Biosystem transmission electron microscope. Histology was assessed qualitatively and quantitatively.

3.3.1 Axon counts and g-ratios

Electron microscope (EM) images, of 0.01 mm^2 areas, were sampled from four equidistant quadrants of the optic nerve (Figure III-3A). The number of myelinated and unmyelinated axons were counted from each of the four quadrants using ImageJ (<http://imagej.nih.gov/ij/>; provided in the public domain by the National Institutes of Health, Bethesda, MD, USA). Degenerating axons, and axons not completely within the image area were also not counted. The mean

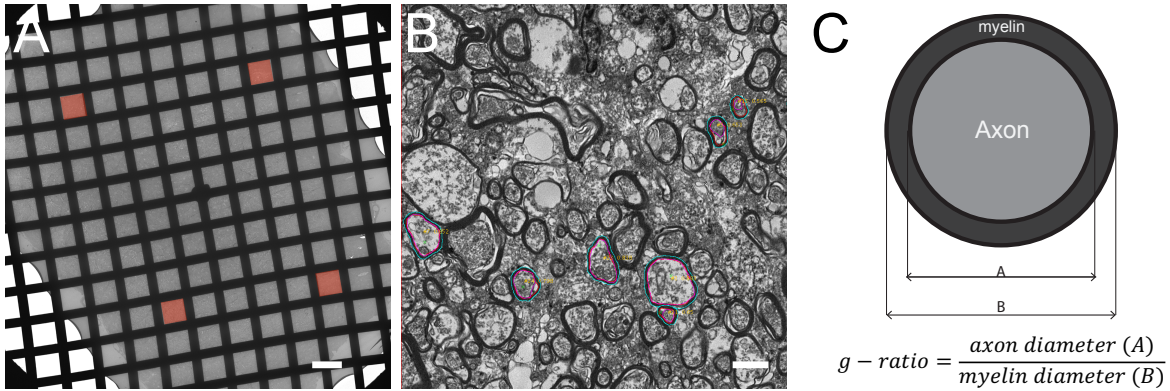


Figure III-3. EM image analysis method. A) Four equidistant quadrants were sampled from both optic nerves. Total myelinated and unmyelinated axons were counted within the sampled area. B-C) For each of the four sampled quadrants, g-ratios were calculated for 25 randomly selected axons using ImageJ.

percentage of myelinated:unmyelinated axons were calculated for each quadrant and averaged. The mean g-ratio, which consists of the axon diameter/myelin diameter, of 25 randomly selected axons from each of the four quadrants (total axons measured = 100) were also averaged and calculated using a modified version of an ImageJ plugin (Goebbels *et al.*, 2010). Axons were randomly selected by the plugin, by randomly placing a cross on the image. If the cross fell within an axon, its g-ratio was determined. This version of the ImageJ plugin allows the user to trace the area of the oligodendrocyte inner tongue if present, thus allowing for a more accurate calculation of the axon and myelin diameter (Figure III-3). The axon diameters were compared across the three groups. Lastly, the number of astrocytes within each of the four quadrants were also counted and compared across the three treatment groups.

3.4 Western blots and ELISAs

Blood from the left cardiac ventricles of KYNA-infused (n = 6), PBS-infused (n = 5) and negative control (n = 6) chicks were collected into 5 ml syringes using a 23G needle, and aliquoted into 1.5 mL Eppendorf tubes prior to injecting the 100 IU of heparin. The tubes were

left undisturbed for 30 minutes before centrifuging at 2000xg for 10 minutes to separate the serum. Serum was then collected and stored at -80°C until assayed. The tissues of the brain and optic nerve were removed carefully and stored at -80°C until assayed. During the dissection, nerves were inspected to confirm the location of the catheter within the nerve.

Enzyme-linked immunosorbent assay (ELISA) kits for anti-chicken proteolipid protein-1 (PLP1; LS-F14513, Cedarlane, Burlington, Ontario) and anti-chicken myelin basic protein (MBP; LS-F14742, Cedarlane, Burlington, Ontario) were used to determine the concentration of these respective proteins in the animal serum. Serum samples were not diluted and were tested in quadruplicate for both ELISAs. Plates were read on a SpectraMax M5 (Molecular Devices, Sunnyvale, CA, USA) using SoftMax® Pro 5 (Molecular Devices, Sunnyvale, CA, USA) software. The SoftMax® Pro 5 software was also used to determine the best-fit equation for the standard curve based on the ELISA kits recommended fit. For the PLP1 ELISA assay a four-parameter logistic curve was determined, $y = \frac{(A-D)}{1+(\frac{x}{C})^B} + D$, while a linear equation was used for the MBP ELISA assay, $\log(y) = A + B * \log(x)$, with R² values of 0.99 for both equations.

Optic nerves of KYNA-infused (n = 4), PBS-infused (n = 4) and negative control (n = 4) chicks were washed with ice-cold PBS and sonicated on ice using a Branson Sonifier 450 (VWR, Mississauga, Ontario, Canada) in an ice-cold sample buffer cocktail containing 50 mM Tris, pH 6.8, 2.5% glycerol, 5% SDS (71736, Sigma-Aldrich, Oakville, Ontario), 4M urea with Protease Inhibitor Cocktail (P8340, Sigma-Aldrich, Oakville, Ontario) and Phosphatase Inhibitor Cocktails (P2850 and P5726, Sigma-Aldrich, Oakville, Ontario). The homogenate was then centrifuged at 10000xg for 15 min at 4°C. The supernatant was transferred and the protein concentration was measured using a DC Protein Assay Kit II (5000122, Bio-Rad Laboratories,

Mississauga, Ontario) with a SpectraMax M5 (Molecular Devices, Sunnyvale, CA, USA) spectrophotometer. The protein concentrations were equalized by adding additional sample buffer cocktail. 15 µg of protein from each sample was aliquoted into separate tubes with an equal volume of sample buffer cocktail with 0.01% bromophenol blue and 10mM Dithiothreitol (DTT; 1610610, Bio-Rad Laboratories, Mississauga, Ontario). Samples were boiled for 5 minutes at 95 °C prior to loading the gel wells. A dual colour standard (1610374, Bio-Rad Laboratories, Mississauga, Ontario) was used as a ladder.

Protein samples were separated by SDS-PAGE using 12% Mini-Protein TGX Precast Protein Gels (4561046DC, Bio-Rad Laboratories, Mississauga, Ontario) at 200 V for 45 minutes in the Bio-Rad Mini-Protean System (165-8000, Bio-Rad Laboratories, Mississauga, Ontario). Each gel was transferred to a 0.2 µm Immun-Blot PVDF membranes (1620174, Bio-Rad Laboratories, Mississauga, Ontario) for 45 mins at 100 V. Transfer of the proteins was confirmed by flooding the PVDF membrane with a Ponceau S staining solution for 1 hour at room temperature. The Ponceau S stain was then washed out completely with distilled deionized water.

Blocking for nonspecific binding was performed with 5% skim milk in Tris-Buffered Saline (1706435, Bio-Rad Laboratories, Mississauga, Ontario) containing 0.01% Tween 20 (TTBS) for 1 hour at room temperature. Membranes were incubated overnight at 4°C with primary antibodies for MBP, PLP, MAG and GFAP (Table III-1) diluted in blocking solution. MAG primary antibodies were used to probe against membranes obtained from non-reducing gels. Blots were then washed with TTBS three times for 10 minutes each at room temperature with gentle agitation. Membranes were then incubated with the appropriate secondary horse radish peroxidase (HRP) conjugated antibody (Table III-1), diluted in the same blocking

solution, for 1.5 hours at room temperature, followed by washing in TTBS three times for 10 minutes each at room temperature. Membranes were then treated with Amersham ECL Western Blotting Chemiluminescence Detection Reagent (GERPN223, Sigma-Aldrich, Oakville, Ontario) for 5 minutes and photographed using a Nikon T2i SLR camera (courtesy of Varadhu Jayakumar) with a 60 second exposure time.

The above membranes were then stripped with Restore Western Blot Stripping Buffer (21059, ThermoFisher Scientific, Burlington, Ontario) and washed with TTBS three times for 10 minutes each. Membranes were blocked as above and incubated overnight at 4°C with primary anti- β -actin (Table III-1) as a loading control. Membranes were washed again as above and incubated with the appropriate secondary HRP antibody (Table III-1) for 1.5 hour at room temperature. The membranes were washed in TTBS and treated with Amersham ECL Western Blotting Chemiluminescence Detection Reagent for 5 minutes and photographed as above.

Table III-1. Primary and secondary antibodies used for western blot analysis.

Type	Antigen	Host	Dilution	Source
Primary	MBP	Rat	1:2000	MAB386, EMD Millipore
	PLP	Rabbit	1:1000	ab105784, abcam
	MAG	Mouse	1:500	MAB1567, EMD Millipore
	GFAP	Mouse	1:500	G3893, Sigma-Aldrich
	b-actin	Mouse	1:1000	ab8224, abcam
Secondary	Rat IgG HRP	Goat	1:30000 (MBP)	ab97057, abcam
	Rabbit IgG HRP	Goat	1:30000 (PLP)	ab6721, abcam
	Mouse IgG HRP	Rabbit	1:20000 (MAG, b-actin, GFAP)	ab97046, abcam

The specific bands were compared by densitometry analysis using ImageStudioLite software (LI-COR Biosciences, Lincoln, NE, USA). Protein levels for the markers of interest were normalized against β -actin levels.

3.5 Statistical analysis

For the percent of myelinated axons, g-ratios, axon diameters and western blot data, a 2x3 mixed model ANOVA (Statistica 8.0, Statsoft, Boston, MA, USA) was used to determine differences between eyes (treated vs control) and treatment groups (KYNA-infused, PBS-infused, and no treatment). Tukey-HSD post hoc tests were used to determine any differences between treatment groups. Bonferroni post hoc tests were used to determine any differences between eyes. ELISA data were analysed using a one-way ANOVA to determine differences between treatment groups. Kruskal-Wallis ANOVAs were used to compare astrocyte cell counts across treatment groups for each eye. For all tests, differences were considered significant if $P < 0.05$. All means are reported with the standard deviation unless otherwise noted.

IV: RESULTS

4.1 Histology and electron microscopy

The chick optic nerve is an ovoid structure that contains prominent pial vasculature with thick walls, oligodendrocytes, astrocytes and a mixture of large myelinated axons and numerous clusters of small diameter unmyelinated axons (Figure III-3) Although the infusion of PBS had no effect on the histological appearance of the optic nerve (Figure IV-2), the infusion of KYNA resulted in a remarkable loss of myelin sheaths and an increase in the number of glial cells (Figure IV-3). Infusion of 50 mM of KYNA for 1 week resulted in large areas of myelin loss with no inflammatory response, preservation of normal morphology of most axons, astrogliosis and evidence of axonal degeneration in a small number of axons. The contralateral optic nerve of KYNA-infused chicks had some myelin loss, but not to the extent of the implanted nerve (Figure IV-3).

The mean percent of myelinated axons was not statistically different between the treatment groups ($p = 0.0936$) or between the eye ($p = 0.0537$). No interaction between the eyes and treatment group was observed ($p = 0.1852$). However, the data for the percent of myelinated axons from the treated eye (left eye) violates the assumption of homogeneity of variances (Levene's test, $p = 0.0012$) and likely affects the results of the statistical test. Also, a lack of power for the treatment ($p = 0.4599$), eye ($p = 0.5042$) and interaction ($p = 0.3222$) effects likely compromise the results of this ANOVA. It appears 3 out of the 7 treated optic nerves from KYNA-infused birds were seemingly unaffected by the treatment resulting in a bimodal distribution within this subset of the data (Figure IV-4A). A greater sample size may be required to demonstrate a significant statistical effect. However, mean g-ratios were statistically different across treatment groups ($p = 0.0037$) and between eyes ($p = 0.0005$; Figure IV-4B).

Irrespective of the eye, mean g-ratios for KYNA-infused chicks were greater than those for negative control birds (0.86 ± 0.04 for KYNA vs 0.78 ± 0.02 for NC; $p = 0.0029$) but were not significantly greater than compared to PBS-infused chicks (0.83 ± 0.06 ; $p = 0.2605$). Mean g-ratios for PBS-infused birds were also not significantly different than those for negative control birds (0.83 ± 0.06 for PBS vs 0.78 ± 0.02 for NC; $p = 0.1333$). Axon diameters were not statistically different across treatment groups ($p = 0.7500$) nor between eyes ($p = 0.9204$) nor as an interaction between treatment groups and eyes ($p = 0.8500$; Figure IV-5A). A main effect in the left eye, across treatment groups, was found for the mean number of astrocytes ($p = 0.0329$), however no post-hoc differences were found within the left eye ($p > 0.1449$). Meanwhile, the right eye was not statistically different across treatment groups ($p = 0.5533$).

4.2 ELISA and western blots

The concentrations of both PLP1 and MBP, in the chick serum, were not dependent on the treatment group ($p = 0.8759$ and $p = 0.8330$, respectively; Table IV-1). On the other hand, qualitative differences were observed in the western blots for the various proteins of interest (Figure IV-6A). Bands for both isoforms of MBP, and PLP showed qualitatively reduced levels in KYNA-infused birds compared to PBS-infused and negative control birds. Moreover, the implanted eye qualitatively appeared to have a further reduction of these myelin proteins compared to the contralateral optic nerve. A statistically significant interaction effect was detected for MBP 1 (20 kDa isoform), MBP 2 (12 kDa isoform) and PLP ($p = 0.0113$, $p = 0.0063$, $p = 0.0461$, respectively), however, no post-hoc significant effects were detected, nor were there any main effects across treatment groups ($p = 0.0914$, $p = 0.5749$, $p = 0.3592$, respectively), nor a main effect between eyes ($p = 0.0563$, $p = 0.9431$, $p = 0.5351$, respectively). MAG did not appear to qualitatively demonstrate a similar reduction in KYNA-infused birds

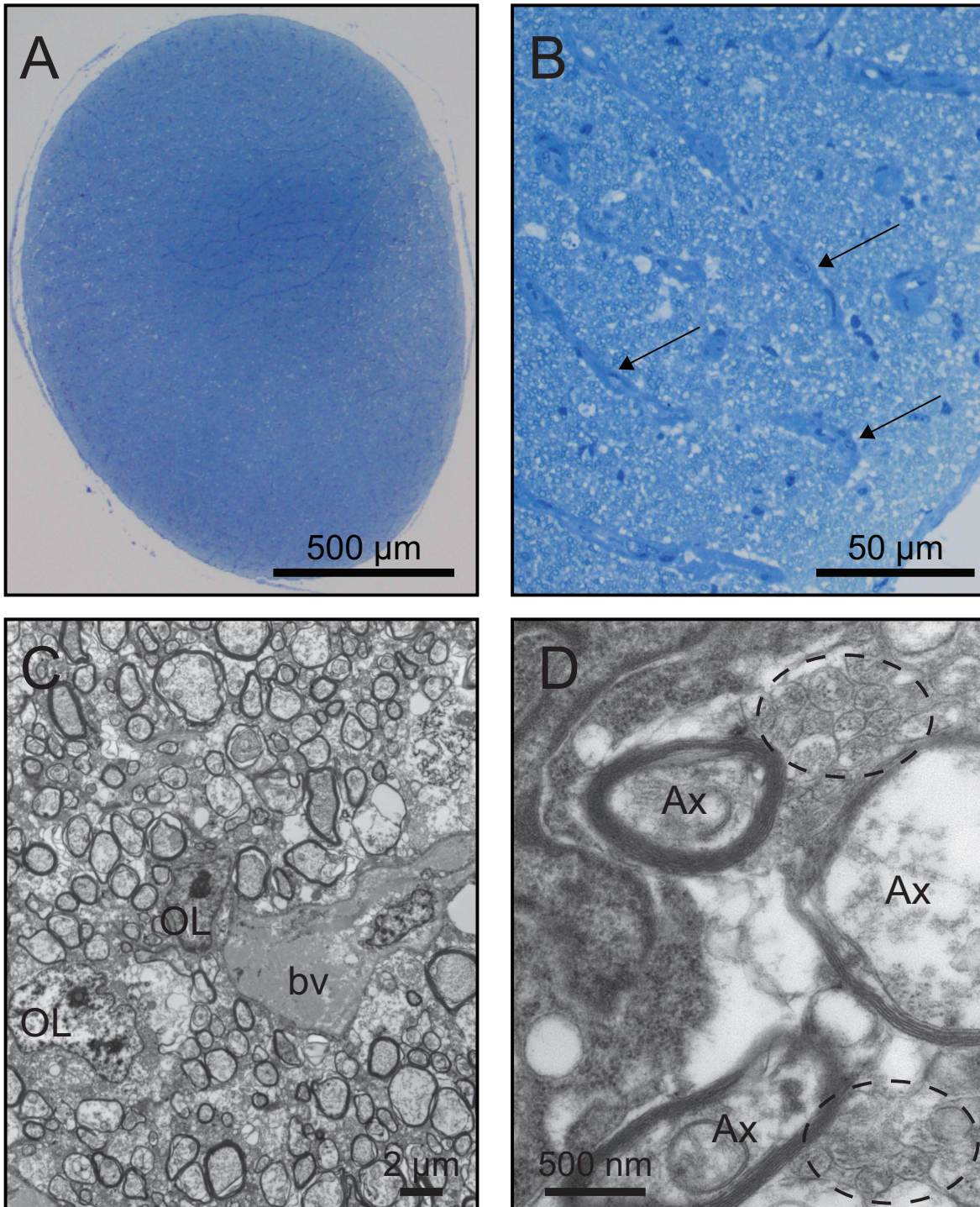


Figure IV-1. Morphology and features of the normal chicken optic nerve. A-B) Toluidine blue stained cross-section of a 14-day old normal chick optic nerve. Arrows indicate the thick pial vasculature visualized by dark staining regions on the chick optic nerve. C-D) EM cross-section of a 14-day old normal chick optic nerve blood vessel (bv), oligodendrocyte (OL), axon (Ax) and population of unmyelinated axons (dashed circle).

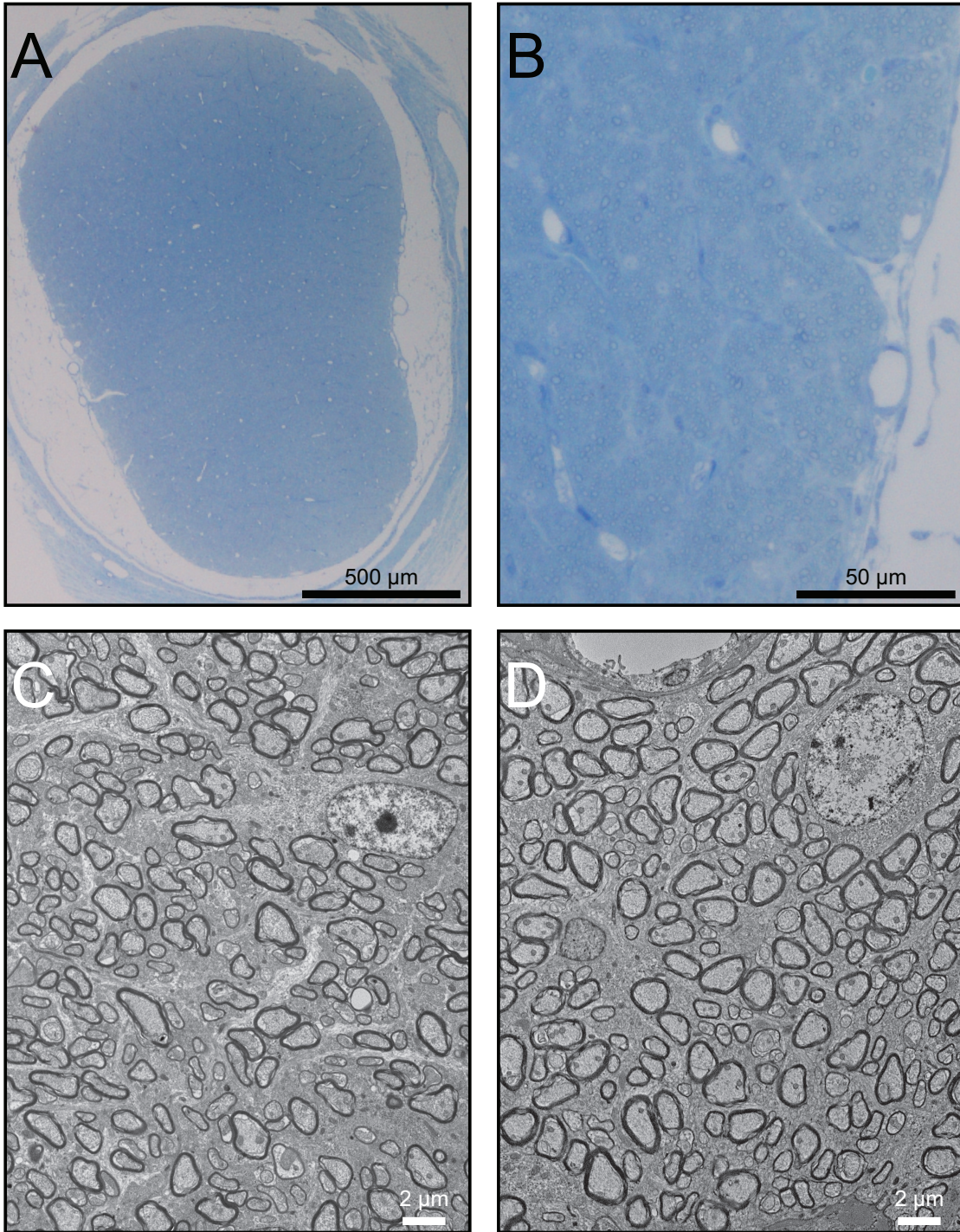


Figure IV-2. Effect of subdural infusion on the implanted and contralateral optic nerves for PBS-infused chicks. A-B) Toluidine blue and EM (C-D) images for PBS infused nerves. Both the implanted nerve (C) and contralateral nerve (D) showed little to no myelin loss.

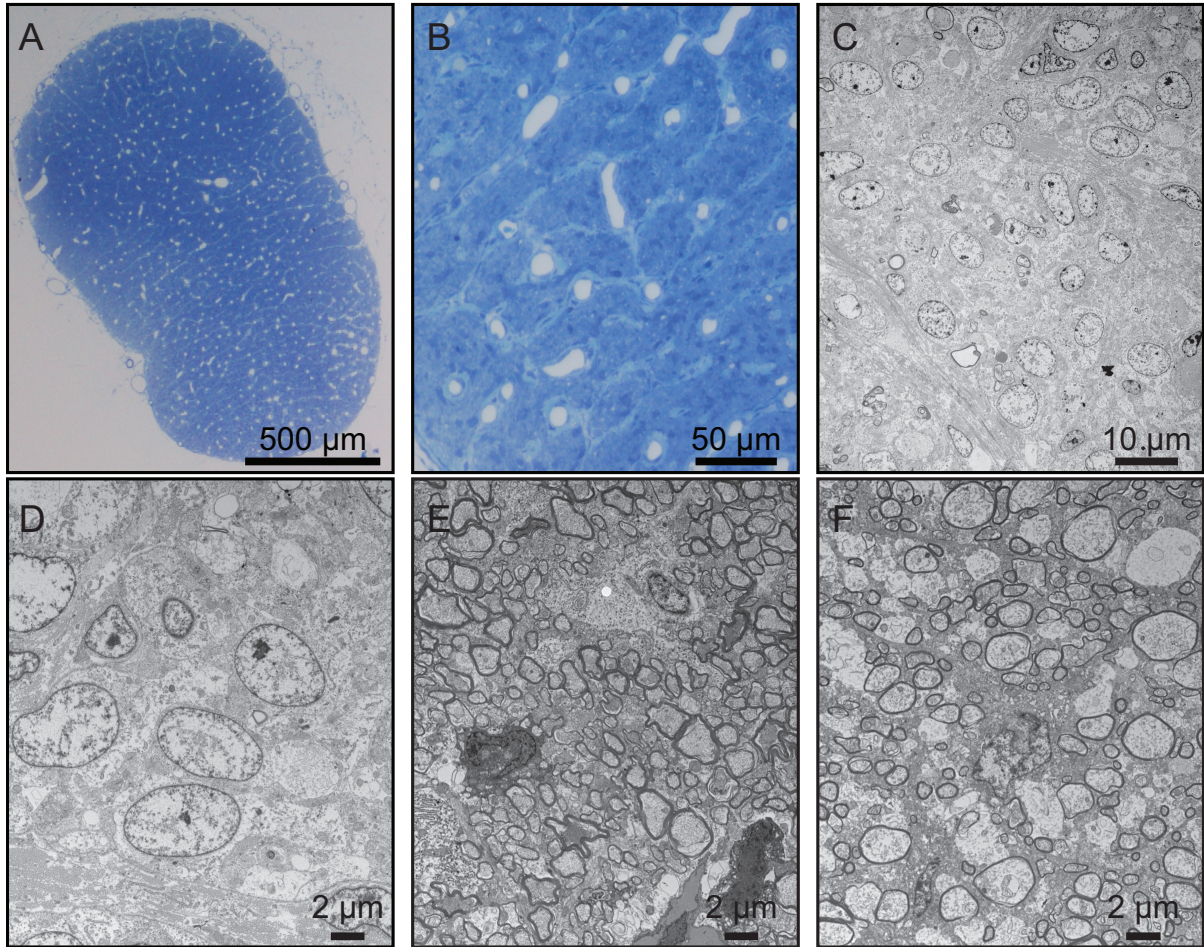


Figure IV-3. Effect of subdural infusion on the implanted and contralateral optic nerves for KYNA-infused chicks. A-B) Toluidine blue and EM (C-F) images for KYNA-infused nerves. The implanted nerve (A-D) showed severe myelin loss. The contralateral nerve (E-F) exhibited some localized regions of myelin loss (F).

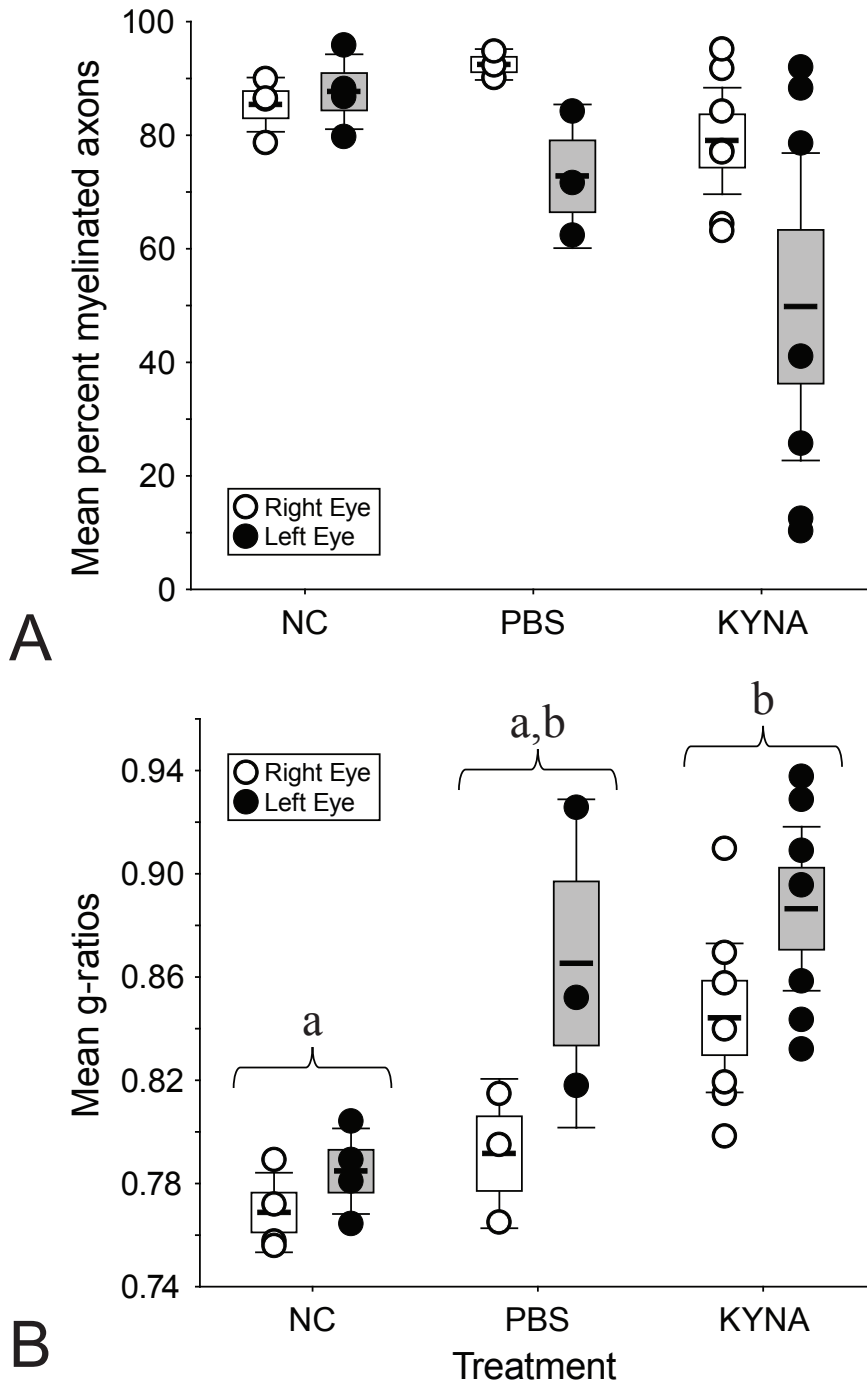


Figure IV-4. Mean percent of myelinated axons (A,) and mean g-ratios (B) for negative control (NC), PBS-infused and KYNA-infused birds. Groups denoted by the same letter(s) are not significantly different. Middle bar represents the mean. Box value represents 1 standard error and the whiskers represent 2 standard errors.

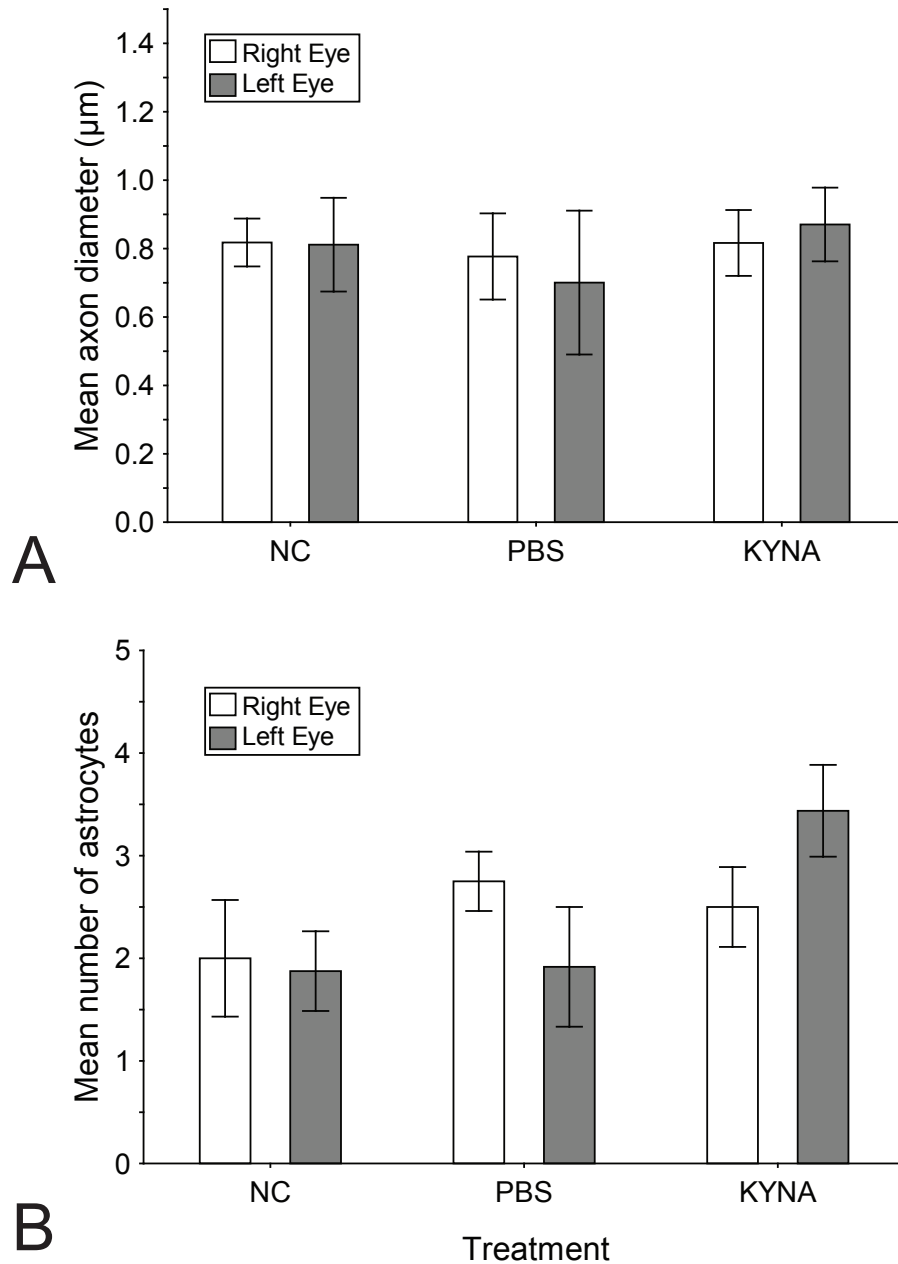


Figure IV-5. Mean axon diameter (A) and mean number of astrocytes (B) for both eyes across negative control (NC), PBS-infused, and KYNA-infused birds. Mean axon diameters were not different across treatment groups ($p = 0.7500$). A main effect in the left eye was detected for the mean number of astrocytes ($p = 0.0329$). Bars represent mean \pm SE.

compared to either the PBS-infused and negative control birds. The relative intensities for MAG were also not dependent on the treatment group ($p = 0.4610$) nor which eye ($p = 0.6190$) nor was an interaction effect detected ($p = 0.2630$). Interestingly, qualitatively, GFAP appeared to be elevated in the PBS-infused nerves compared to either the KYNA-infused or negative control birds, however, these differences were not statistically significant. Relative GFAP intensities were not dependent on the treatment group ($p = 0.3942$) nor which eye ($p = 0.3999$) nor was an interaction effect detected ($p = 0.1079$).

Table IV-1. Mean serum concentrations of PLP1 and MBP for KYNA-treated, PBS-treated and negative control birds.

Treatment Group	PLP1 (ng/ml)	MBP (ng/ml)
KYNA (n=6)	0.75 ± 0.23	1.26 ± 0.11
PBS (n=5)	0.76 ± 0.19	1.28 ± 0.07
negative controls (n=6)	0.81 ± 0.21	1.30 ± 0.11

The concentrations of PLP1 and MBP, in the chick serum, were not dependent on the treatment group ($p = 0.8759$ and $p = 0.8330$, respectively)

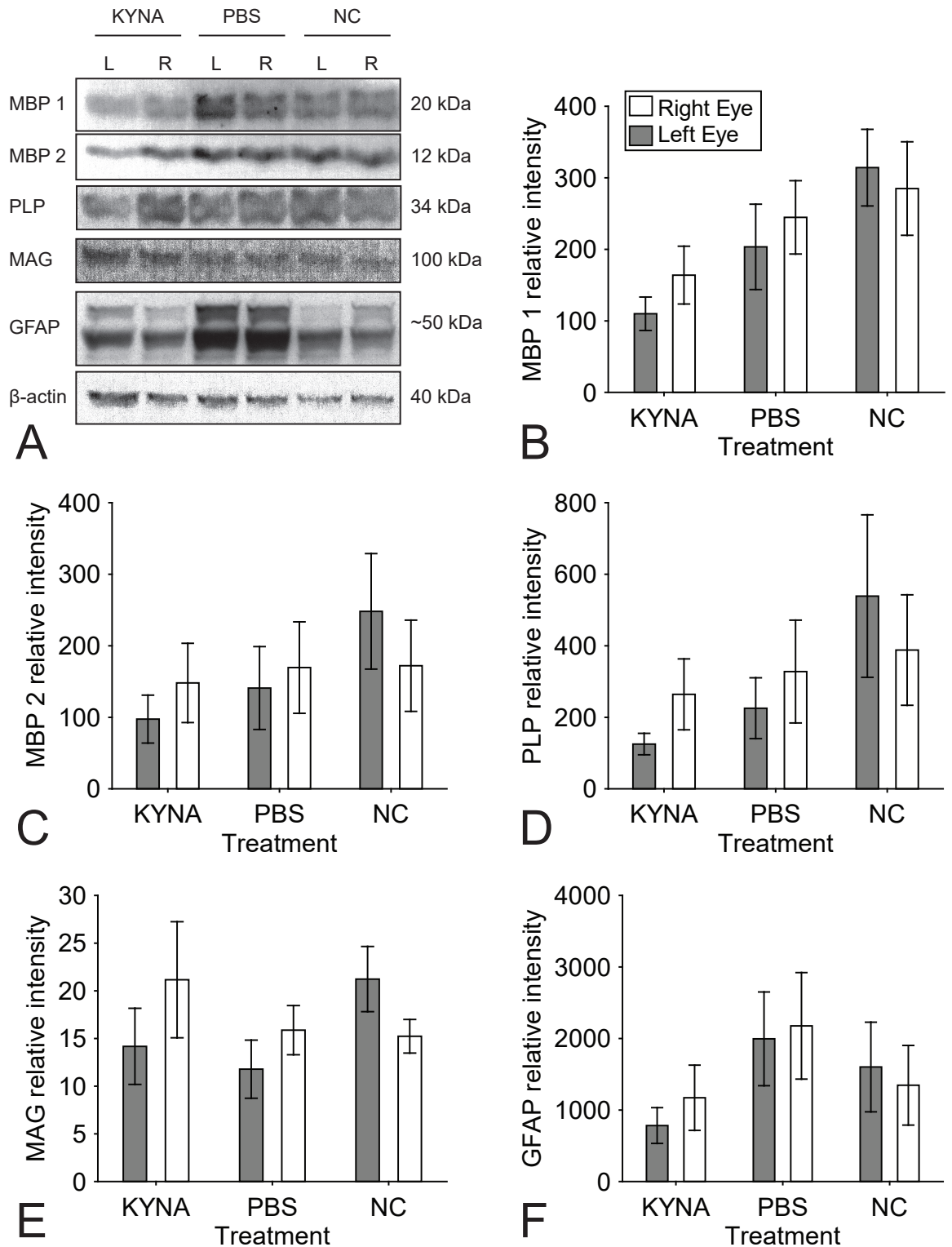


Figure IV-6. Semi-quantitative analysis of western blots data. A) Representative western blots of the left (L) and right (R) eyes for KYNA-infused, PBS-infused and negative control (NC) birds. B-F) Band intensities as a percent relative to β -actin levels, for each of the treatment groups. Bars represent mean \pm SE.

V: DISCUSSION

The method used in the following experiments, to deliver KYNA to the optic nerve *in vivo*, has not been previously reported in a chicken model. A similar method, using implanted ALZET osmotic pumps in New Zealand White rabbit optic nerves, has been used to deliver isoproterenol (Hodges-Savola *et al.*, 1996) and kainate (Matute *et al.*, 1997; Soto *et al.*, 2004) through continuous infusion. However, the implantation procedure performed by these groups involve dissection of the superior extraocular muscles. Unlike the chicken, the rabbit optic nerve, like that of other mammals, has a central retinal artery (May, 2008). Both dissection of the muscles and the presence of the central retinal artery provide reasons to opt for the chicken model. The Dissection of the muscles may have an effect on the development and growth of the eye by deregulating binocular vision and altering the biomechanical properties of the eyeball (Greene, 1981; Zhou *et al.*, 2011). Moreover, inserting a catheter for infusion of the compound of interest may affect blood flow in the optic nerve, introducing the possible ischaemic effects. Our surgical procedure indicates successful delivery of an agent, over 7 days. The presence of India ink in the surgically treated nerve, the contralateral nerve, and the optic chiasm indicates a wide distribution of the delivered agent (Figure III-2). However, it is unclear if the distribution of the agent is equal across the entire visual pathway. Given the that catheter is placed in the left nerve, it's likely the left nerve receives a greater amount of the delivered agent than the other structures. It is also unclear to what extent the compound spreads through the visual pathway and the rest of the brain. Given that no obvious dark staining was observed beyond the chiasm it is likely that any agents that reach these areas are negligible in dose and consequently its effect. It's also possible that some of the agent flows into the eye, possibly affecting the retina. Unlike other animals, chicken retinas contain oligodendrocytes and are consequently myelinated during

embryonic development (Nakazawa *et al.*, 1993). Subsequently, administration of KYNA could have had an effect on the degree of myelination within the retina and subsequently effect the downstream pathway. Confirmation of any effect of KYNA on the retina, through administration via the optic nerve, would need further study. That the negative control and PBS-infused visual pathways have a similar appearance suggests that the surgical procedure does not result in severe or permanent damage to these tissues. The lack of major superficial damage provides further reason to use this surgical method to deliver agents to the optic nerve, without the need for dissecting extraocular muscles.

Histological images obtained from negative control, PBS-infused, and KYNA-infused birds revealed remarkable differences. As expected, KYNA-infused birds demonstrated a remarkable loss of myelin while preserving normal axonal morphology (Figure IV-3). Additionally, a surprising number of reactive astrocytes were present in KYNA-infused electron micrographs. In contrast, both the PBS-infused and negative control bird's electron micrographs appeared similar with no remarkable changes in the level or appearance of myelinated axons, or the number of astrocytes (Figure IV-2). None of the toluidine blue stained images or electron micrographs for any of the treatment groups showed signs of inflammatory infiltration. These data correspond well to a previous study by Dabrowski and colleagues (2015) in which KYNA-infused rat spinal cords demonstrated similar effects and did not lead to inflammation. A recent study by Langner and colleagues (2017) has also revealed that high concentrations of KYNA affect the viability and metabolic activity of oligodendroglial cells *in vitro* but did not have an effect on the oligodendroglial cell proliferation and morphology. Langner and colleagues (2017) also demonstrated the effect of KYNA to be independent of its role as a glutamate receptor antagonist. Consequently, the mechanism by which KYNA affects oligodendrocytes and their

ability to wrap axons with myelin may be related to its role as an $\alpha 7$ nicotinic acetylcholine ($\alpha 7$ nACh) receptor antagonist or G-protein-coupled receptor 35 (GPR35) agonist. Expression of GPR35 mRNA has been observed in rat spinal cords and dorsal root ganglion (Ohshiro *et al.*, 2008) as well as in mouse astrocytes (Berlinguer-Palmini *et al.*, 2013). Furthermore, KYNA may induce the production of inositol phosphate and elicit Ca^{2+} mobilization (Divorty *et al.*, 2015). Studies have suggested that GPR35 can modulate inflammatory conditions. Through the GPR35 receptor, agonists like kynurenic acid have been demonstrated to attenuate inflammatory processes and inhibit the release of tumor necrosis factor α (Wang *et al.*, 2006; Kuc *et al.*, 2008; Barth *et al.*, 2009; Thorburn *et al.*, 2014). These additional attributes in conjunction or separately may be involved in the mechanism by which myelin loss is occurring.

The non-significant differences between the percent of myelinated nerve fibers across treatment groups was unexpected. However, it is likely that the lack of significance was due to the binomial distribution of data within the left eye of the KYNA-treated nerves (Figure IV-4A). Three out of the seven KYNA-infused birds did not demonstrate the same proportion of axons with total myelin loss as the other birds (Figure IV-4A). It is unclear why these three birds were less affected by administration of KYNA. It is possible that the surgery was not successful in these three birds, although, during dissection of the nerves, the location and presence of the catheter is confirmed. Moreover, the pumps were inspected to ensure there was no residual volume left over. Nonetheless, it's conceivable that the variations in the location or perfusion characteristics produced lower delivery to the target organ. Also, it's possible that damage to the sheath on the opposite side of the nerve led to another point of drainage, also leading to inadequate delivery of the agent to the nerve. Although the percent of myelinated axons varied for KYNA-infused birds, a more consistent effect on axon g-ratios indicates an overall change in

the degree of myelination. The g-ratios provide a more robust means of analyzing the effect of PBS or KYNA on the optic nerves compared to negative controls. An inability to determine statistical differences in g-ratios between eyes of the three treatment groups suggests that agent delivery occurs in substantial amounts across the nerves and chiasm resulting in proportional effect on both nerves. The slightly larger g-ratios in the left eyes, for both PBS- and KYNA-infused birds, may also be associated with damage inflicted by the surgical procedure (Figure IV-4). Given that a foreign object is being implanted in the nerve for 7 days, and CSF is being displaced by PBS or KYNA diluted in PBS, it is likely that this damaging effect is responsible for the larger g-ratios. That axon diameters revealed no significant differences indicates a direct change in the degree of myelination, while axonal morphology was unaffected (Figure IV-5A). As noted in electron micrographs, KYNA-infused birds displayed astrogliosis as characterized by a difference in the mean number of astrocytes in the implanted nerves (Figure IV-5B).

That no significant difference was found, between the concentration of serum MBP and PLP-1 for the three treatment groups, suggests that the mechanism of myelin loss is non-destructive in nature (Table IV-1). Other studies have demonstrated that in patients suffering from traumatic brain injury (TBI), MBP concentrations in serum were elevated and strongly correlated with the severity of the injury (Thomas *et al.*, 1978; Berger *et al.*, 2007). Moreover, neurologically impaired patients, such as those with demyelinating and encephalitic diseases have also demonstrated elevated serum concentrations of PLP (Trotter *et al.*, 1983) and MBP (Ohta *et al.*, 2002). Antibodies against myelin proteins are also elevated in the serum of relapsing-remitting MS patients (Angelucci *et al.*, 2005). These neurological injuries involve a destructive and damaging mechanism leading to elevated concentrations of myelin proteins in the patient serum. In contrast, due to the non-inflammatory nature of the KYNA-associated

myelin loss, myelin from the optic nerve is likely not being damaged or destroyed but retracted through its effects on oligodendrocytes.

A qualitative decrease in the MBP isoforms and PLP in KYNA-infused birds correlates well with the elevated g-ratios in the electron microscopy images. Moreover, given that there is a qualitative reduction in these proteins in the optic nerve, without an elevation of these proteins in serum, further suggests a non-destructive, non-inflammatory nature of myelin loss. The lack of a qualitative decrease of MAG in the KYNA-infused birds was surprising given that the other myelin proteins showed slight decreases. However, unlike MBP or PLP, MAG has key functions in myelin maintenance. MAG acts as both a ligand for the axonal NgR receptor and as a receptor for axonal signalling that promotes differentiation, maintenance and the survival of oligodendrocytes (Quarles, 2007). In CNS MAG-deficient mice, the initiation of myelination, formation of intact myelin sheaths and the integrity is affected. Thus, it is possible that MAG expression is modulated in response to the KYNA-associated myelin loss, as a means of counteracting KYNAs' effects on the viability of oligodendrocytes within the nerve. Injury to the brain and CNS tissue triggers astrocytes to become reactive, which involves the upregulation of GFAP and changes in astrocyte morphology (Vanezis *et al.*, 1987; Hatten *et al.*, 188). Indeed, glaucoma models in mice have also demonstrated an elevated expression of GFAP in western blots of optic nerves (Joos *et al.*, 2010; Sun *et al.*, 2013). The elevation of GFAP was a consequence of the injury to the retinal ganglion cells via intraocular pressure elevation. Subsequently, the observation that GFAP was elevated in PBS-infused nerves was expected given the traumatic and injury-inducing nature of the surgical implant. However, given that KYNA-infused birds underwent the same surgical procedure and appeared to have a greater amount of astrogliosis, the lack of elevated GFAP in these birds seems contradictory. Through

KYNA's agonistic interaction with the GPR35 receptor located on astrocytes of the CNS, a reduction of intracellular cyclic adenine monophosphate (cAMP) has been demonstrated (Berlinguer-Palmiini *et al.*, 2013). Elevated intracellular cAMP is required for the induction of GFAP expression in astrocytes (Roymans *et al.*, 2001). Therefore, it is plausible that KYNAs inhibition of intracellular cAMP may be subsequently modulating the expected increase in GFAP expression. Furthermore, the anti-inflammatory properties of KYNA may also further diminish the activation of GFAP in astrocytes. That a statistical difference was not detected, between the treatment groups for western blot proteins, is likely due to the low sample size and consequently low power of the statistical tests. Moreover, the effects of infusion on these birds seemed to have more robust effects in localized regions of the nerve. Hence, a semi-quantitative western blot analysis of the entire optic nerve may not be sensitive enough to detect overall changes in the nerve.

In summary, infusion of KYNA into the implanted optic nerves of chickens was associated with myelin loss. The myelin loss, characterized by changes in axon g-ratios and western blots of the optic nerve indicate an overall reduction in the level of major myelin components, MBP and PLP. A lack of: a histological inflammatory response, a change in serum myelin concentration, and an elevation of GFAP indicates an inflammation suppressing effect of KYNA that could be useful as a tool for regeneration. However, further studies are required to elucidate the long-term effects of administration of KYNA. Oligodendrocyte and myelin revival are essential for complete recovery after injury to CNS tissue. Thus, determining the optimal concentration of KYNA to induce myelin loss and suppress inflammation after injury, is required to ensure an appropriate recovery time for the tissue and oligodendrocytes. The functional effects of administration of KYNA have yet to be determined. Administration of KYNA into the

retina and optic nerves of chickens may be a useful method to study the functional deficits that occur after myelin loss.

LETTERS OF COPYRIGHT PERMISSIONS

FIGURE I-3

Gmail - Thank you for your order with RightsLink / Elsevier

2017-09-21, 7:42 PM



Akshay Gurdita <gurditaakshay@gmail.com>

Thank you for your order with RightsLink / Elsevier

1 message

no-reply@copyright.com <no-reply@copyright.com>
To: Akshay Gurdita <agurdita@uwaterloo.ca>

Mon, Jun 19, 2017 at 3:12 PM



Thank you for your order!

Dear Mr. Akshay Gurdita,

Thank you for placing your order through Copyright Clearance Center's RightsLink® service.

Order Summary

Licensee: University of Waterloo
Order Date: Jun 19, 2017
Order Number: 4132641203151
Publication: Advanced Drug Delivery Reviews
Title: Peripheral nerve regeneration: Experimental strategies and future perspectives
Type of Use: reuse in a thesis/dissertation
Order Total: 0.00 CAD

View or print complete [details](#) of your order and the publisher's terms and conditions.

Sincerely,

Copyright Clearance Center

FIGURE I-4

Gmail - Thank you for your order with RightsLink / Nature Publishing Group

2017-09-21, 7:38 PM



Akshay Gurdita <gurditaakshay@gmail.com>

Thank you for your order with RightsLink / Nature Publishing Group

1 message

no-reply@copyright.com <no-reply@copyright.com>
To: Akshay Gurdita <agurdita@uwaterloo.ca>

Thu, Jun 22, 2017 at 8:07 PM



Thank you for your order!

Dear Mr. Akshay Gurdita,

Thank you for placing your order through Copyright Clearance Center's RightsLink® service.

Order Summary

Licensee:	University of Waterloo
Order Date:	Jun 22, 2017
Order Number:	4134471357120
Publication:	Nature Reviews Neuroscience
Title:	Glial inhibition of CNS axon regeneration
Type of Use:	reuse in a dissertation / thesis
Order Total:	0.00 CAD

View or print complete [details](#) of your order and the publisher's terms and conditions.

Sincerely,

Copyright Clearance Center

How was your experience? Fill out this [survey](#) to let us know.

FIGURE I-6

Gmail - Thank you for your order with RightsLink / Elsevier

2017-09-21, 7:31 PM



Akshay Gurdita <gurditaakshay@gmail.com>

Thank you for your order with RightsLink / Elsevier

1 message

no-reply@copyright.com <no-reply@copyright.com>
To: Akshay Gurdita <agurdita@uwaterloo.ca>

Thu, Jun 22, 2017 at 7:58 PM



Thank you for your order!

Dear Mr. Akshay Gurdita,

Thank you for placing your order through Copyright Clearance Center's RightsLink® service.

Order Summary

Licensee: University of Waterloo
Order Date: Jun 22, 2017
Order Number: 4134470856311
Publication: Developmental Biology
Title: Molecular mechanisms of optic vesicle development: Complexities, ambiguities and controversies
Type of Use: reuse in a thesis/dissertation
Order Total: 0.00 CAD

View or print complete [details](#) of your order and the publisher's terms and conditions.

Sincerely,

Copyright Clearance Center

FIGURE I-8



Council

David R. Sibley
President
Bethesda, Maryland

John D. Schuetz
President-Elect
St. Jude Children's Research Hospital

Kenneth E. Thummel
Past President
University of Washington

Charles P. France
Secretary/Treasurer
The University of Texas Health
Science Center at San Antonio

John J. Tesmer
Secretary/Treasurer-Elect
University of Michigan

Dennis C. Marshall
Past Secretary/Treasurer
Ferring Pharmaceuticals, Inc.

Margaret E. Gnegy
Councilor
University of Michigan Medical School

Wayne L. Backes
Councilor
Louisiana State University Health
Sciences Center

Carol L. Beck
Councilor
Thomas Jefferson University

Mary E. Vore
Chair, Board of Publications Trustees
University of Kentucky

Brian M. Cox
FASEB Board Representative
Uniformed Services University
of the Health Sciences

Scott A. Waldman
Chair, Program Committee
Thomas Jefferson University

Judith A. Siuciak
Executive Officer

June 23, 2017

Akshay Gurdita
School of Optometry
University of Waterloo
200 Columbia St. W
Waterloo, ON N2L 3G1
Canada

Email: agurdita@uwaterloo.ca

Dear Akshay Gurdita:

This is to grant you permission to reproduce the following figure in your dissertation titled "Can kynurenic acid cause myelin loss in chicken optic nerves?" for the University of Waterloo:

Figure FS1 from R Schwarcz and R Pellicciari (2002), Manipulation of Brain Kynurenines: Glial Targets, Neuronal Effects, and Clinical Opportunities, *J Pharmacol Exp Ther*, 303(1):1-10; DOI: <https://doi.org/10.1124/jpet.102.034439>

Permission to reproduce the figure is granted for worldwide use in all languages, translations, and editions, and in any format or medium including print and electronic. The authors and the source of the materials must be cited in full, including the article title, journal title, volume, year, and page numbers.

Sincerely yours,

Richard Dodenhoff
Journals Director

REFERENCES

- Adler, R. and Canto-Soler, M. V. (2007). "Molecular mechanisms of optic vesicle development: complexities, ambiguities and controversies." Developmental Biology **305**(1): 1-13.
- Aguayo, A. J., Vidal-Sanz, M., Villegas-Perez, M. P. and Bray, G. M. (1987). "Growth and connectivity of axotomized retinal neurons in adult rats with optic nerves substituted by PNS grafts linking the eye and the midbrain." Annals of the New York Academy of Sciences **495**: 1-9.
- Aktas, Z., Gurelik, G., Gocun, P. U., Akyurek, N., Onol, M. and Hasanreisoglu, B. (2010). "Matrix metalloproteinase-9 expression in retinal ganglion cell layer and effect of topically applied brimonidine tartrate 0.2% therapy on this expression in an endothelin-1-induced optic nerve ischemia model." International Ophthalmology **30**(3): 253-259.
- Amrite, A. C. and Kompella, U. B. (2005). "Size-dependent disposition of nanoparticles and microparticles following subconjunctival administration." Journal of Pharmacy and Pharmacology **57**(12): 1555-1563.
- Angelucci, F., Mirabella, M., Frisullo, G., Caggiula, M., Tonali, P. A. and Batocchi, A. P. (2005). "Serum levels of anti-myelin antibodies in relapsing-remitting multiple sclerosis patients during different phases of disease activity and immunomodulatory therapy." Disease Markers **21**(2): 49-55.
- Anis, N. A., Berry, S. C., Burton, N. R. and Lodge, D. (1983). "The dissociative anaesthetics, ketamine and phencyclidine, selectively reduce excitation of central mammalian neurones by N-methyl-aspartate." British Journal of Pharmacology **79**(2): 565-575.
- Barth, M. C., Ahluwalia, N., Anderson, T. J., Hardy, G. J., Sinha, S., Alvarez-Cardona, J. A., Pruitt, I. E., Rhee, E. P., Colvin, R. A. and Gerszten, R. E. (2009). "Kynurenic acid triggers firm arrest of leukocytes to vascular endothelium under flow conditions." Journal of Biological Chemistry **284**(29): 19189-19195.
- Bartsch, U., Bandtlow, C. E., Schnell, L., Bartsch, S., Spillmann, A. A., Rubin, B. P., Hillenbrand, R., Montag, D., Schwab, M. E. and Schachner, M. (1995). "Lack of evidence that myelin-associated glycoprotein is a major inhibitor of axonal regeneration in the CNS." Neuron **15**(6): 1375-1381.
- Benfey, M. and Aguayo, A. J. (1982). "Extensive elongation of axons from rat brain into peripheral nerve grafts." Nature **296**(5853): 150-152.
- Berger, R. P., Beers, S. R., Richichi, R., Wiesman, D. and Adelson, P. D. (2007). "Serum biomarker concentrations and outcome after pediatric traumatic brain injury." Journal of Neurotrauma **24**(12): 1793-1801.

Berlinguer-Palmini, R., Masi, A., Narducci, R., Cavone, L., Maratea, D., Cozzi, A., Sili, M., Moroni, F. and Mannaioni, G. (2013). "GPR35 activation reduces Ca²⁺ transients and contributes to the kynurenic acid-dependent reduction of synaptic activity at CA3-CA1 synapses." PLoS One **8**(11): e82180.

Biousse, V. and Newman, N. J. (2015). "Ischemic Optic Neuropathies." New England Journal of Medicine **372**(25): 2428-2436.

Bradbury, E. J., Moon, L. D., Popat, R. J., King, V. R., Bennett, G. S., Patel, P. N., Fawcett, J. W. and McMahon, S. B. (2002). "Chondroitinase ABC promotes functional recovery after spinal cord injury." Nature **416**(6881): 636-640.

Brooks, D. E., Ka'llberg, M. E., Cannon, R. L., Koma`romy, A. M., Ollivier, F. J., Malakhova, O. E., Dawson, W. W., Sherwood, M. B., Kuekuerichkina, E. E. and Lambrou, G. N. (2004). "Functional and Structural Analysis of the Visual System in the Rhesus Monkey Model of Optic Nerve Head Ischemia." Investigative Ophthalmology & Visual Science **45**(6): 1830-1830.

Carson, M. J. (2002). "Microglia as liaisons between the immune and central nervous systems: functional implications for multiple sclerosis." Glia **40**(2): 218-231.

Chauhan, B. C., LeVatte, T. L., Jollimore, C. A., Yu, P. K., Reitsamer, H. A., Kelly, M. E., Yu, D. Y., Tremblay, F. and Archibald, M. L. (2004). "Model of endothelin-1-induced chronic optic neuropathy in rat." Investigative Ophthalmology and Visual Science **45**(1): 144-152.

Connor, T. J., Starr, N., O'Sullivan, J. B. and Harkin, A. (2008). "Induction of indolamine 2,3-dioxygenase and kynurenine 3-monooxygenase in rat brain following a systemic inflammatory challenge: a role for IFN-gamma?" Neuroscience Letters **441**(1): 29-34.

Dabrowski, W., Kwiecien, J. M., Rola, R., Klapek, M., Stanisiz, G. J., Kotlinska-Hasiec, E., Oakden, W., Janik, R., Coote, M., Frey, B. N. and Turski, W. A. (2015). "Prolonged Subdural Infusion of Kynurenic Acid Is Associated with Dose-Dependent Myelin Damage in the Rat Spinal Cord." PLoS One **10**(11): e0142598-e0142598.

David, S. and Aguayo, A. J. (1981). "Axonal elongation into peripheral nervous system "bridges" after central nervous system injury in adult rats." Science **214**(4523): 931-933.

Di Polo, A., Aigner, L. J., Dunn, R. J., Bray, G. M. and Aguayo, A. J. (1998). "Prolonged delivery of brain-derived neurotrophic factor by adenovirus-infected Muller cells temporarily rescues injured retinal ganglion cells." Proceedings of the National Academy of Sciences of the United States of America **95**(7): 3978-3983.

Divorty, N., Mackenzie, A. E., Nicklin, S. A. and Milligan, G. (2015). "G protein-coupled receptor 35: an emerging target in inflammatory and cardiovascular disease." Frontiers in Pharmacology **6**: 41.

Ebadi, M., Bashir, R. M., Heidrick, M. L., Hamada, F. M., Refaey, H. E., Hamed, A., Helal, G., Baxi, M. D., Cerutis, D. R. and Lassi, N. K. (1997). "Neurotrophins and their receptors in nerve injury and repair." Neurochemistry International **30**(4-5): 347-374.

Elkabes, S., DiCicco-Bloom, E. M. and Black, I. B. (1996). "Brain microglia/macrophages express neurotrophins that selectively regulate microglial proliferation and function." Journal of Neuroscience **16**(8): 2508-2521.

Erhardt, S., Blennow, K., Nordin, C., Skogh, E., Lindstrom, L. H. and Engberg, G. (2001). "Kynurenic acid levels are elevated in the cerebrospinal fluid of patients with schizophrenia." Neuroscience Letters **313**(1-2): 96-98.

Erhardt, S. and Engberg, G. (2002). "Increased phasic activity of dopaminergic neurones in the rat ventral tegmental area following pharmacologically elevated levels of endogenous kynurenic acid." Acta Physiologica Scandinavica **175**(1): 45-53.

Faroni, A., Mobasseri, S. A., Kingham, P. J. and Reid, A. J. (2015). "Peripheral nerve regeneration: experimental strategies and future perspectives." Advanced Drug Delivery Reviews **82-83**: 160-167.

Fischer, A. J. and Reh, T. A. (2001). "Muller glia are a potential source of neural regeneration in the postnatal chicken retina." Nature Neuroscience **4**(3): 247-252.

Fischer, A. J. and Reh, T. A. (2002). "Exogenous growth factors stimulate the regeneration of ganglion cells in the chicken retina." Developmental Biology **251**(2): 367-379.

Fischer, D., He, Z. and Benowitz, L. I. (2004). "Counteracting the Nogo receptor enhances optic nerve regeneration if retinal ganglion cells are in an active growth state." Journal of Neuroscience **24**(7): 1646-1651.

Fischer, D. and Leibinger, M. (2012). "Promoting optic nerve regeneration." Progress in Retinal and Eye Research **31**(6): 688-701.

Fitch, M. T. and Silver, J. (2008). "CNS injury, glial scars, and inflammation: Inhibitory extracellular matrices and regeneration failure." Experimental Neurology **209**(2): 294-301.

Fukui, S., Schwarcz, R., Rapoport, S. I., Takada, Y. and Smith, Q. R. (1991). "Blood-Brain Barrier Transport of Kynurenines: Implications for Brain Synthesis and Metabolism." Journal of Neurochemistry **56**(6): 2007-2017.

Gallina, D., Zelinka, C. P., Cebulla, C. M. and Fischer, A. J. (2015). "Activation of glucocorticoid receptors in Muller glia is protective to retinal neurons and suppresses microglial reactivity." Experimental Neurology **273**: 114-125.

Goebbels, S., Oltrogge, J. H., Kemper, R., Heilmann, I., Bormuth, I., Wolfer, S., Wichert, S. P., Mobius, W., Liu, X., Lappe-Siefke, C., Rossner, M. J., Groszer, M., Suter, U., Frahm, J., Boretius, S., Nave, K. A. K.-A., Möbius, W., Liu, X., Lappe-Siefke, C., Rossner, M. J., Groszer, M., Suter, U., Frahm, J., Boretius, S. and Nave, K. A. K.-A. (2010). "Elevated

phosphatidylinositol 3,4,5-trisphosphate in glia triggers cell-autonomous membrane wrapping and myelination." Journal of Neuroscience **30**(26): 8953-8964.

Goldman, D. and Hyde, D. (2014). "Chapter 5 - Restoring Vision to the Blind: Endogenous Regeneration." Translational Vision Science and Technology **3**(7): 7.

Greene, P. R. (1981). "Myopia and the extraocular muscles." Documenta Ophthalmologica **28**: 163-169.

Grove, K., Dobish, J., Harth, E., Ingram, M. C., Galloway, R. L. and Mawn, L. A. (2014). "Trans-meningeal drug delivery to optic nerve ganglion cell axons using a nanoparticle drug delivery system." Experimental Eye Research **118**: 42-45.

Guidetti, P., Luthi-Carter, R. E., Augood, S. J. and Schwarcz, R. (2004). "Neostriatal and cortical quinolinate levels are increased in early grade Huntington's disease." Neurobiology of Disease **17**(3): 455-461.

Guidetti, P., Okuno, E. and Schwarcz, R. (1997). "Characterization of rat brain kynurenine aminotransferases I and II." Journal of Neuroscience Research **50**(3): 457-465.

Guidetti, P. and Schwarcz, R. (1999). "3-Hydroxykynurenine potentiates quinolinate but not NMDA toxicity in the rat striatum." European Journal of Neuroscience **11**(11): 3857-3863.

Guillemin, G. J., Brew, B. J., Noonan, C. E., Takikawa, O. and Cullen, K. M. (2005). "Indoleamine 2,3 dioxygenase and quinolinic acid immunoreactivity in Alzheimer's disease hippocampus." Neuropathology and Applied Neurobiology **31**(4): 395-404.

Guillemin, G. J., Kerr, S. J., Smythe, G. A., Smith, D. G., Kapoor, V., Armati, P. J., Croitoru, J. and Brew, B. J. (2001). "Kynurenine pathway metabolism in human astrocytes: a paradox for neuronal protection." Journal of Neurochemistry **78**(4): 842-853.

Hatten, M. E., Liem, R. K., Shelanski, M. L. and Mason, C. A. (1991). "Astroglia in CNS injury." Glia **4**(2): 233-243.

Hernandez, M. R. (2000). "The optic nerve head in glaucoma: role of astrocytes in tissue remodeling." Progress in Retinal and Eye Research **19**(3): 297-321.

Hodges-Savola, C., Rogers, S. D., Ghilardi, J. R., Timm, D. R. and Mantyh, P. W. (1996). "β-adrenergic receptors regulate astrogliosis and cell proliferation in the central nervous system in vivo." Glia **17**(1): 52-62.

Hodgkin, A. L. and Huxley, A. F. (1952). "A quantitative description of membrane current and its application to conduction and excitation in nerve." Journal of Physiology **117**(4): 500-544.

Hsieh, Y.-c., Chen, R.-f., Yeh, Y.-s., Lin, M.-t., Hsieh, J.-h. and Chen, S.-h. (2011). "Kynurenic acid attenuates multiorgan dysfunction in rats after heatstroke." Acta Pharmacologica Sinica **32**(2): 167-174.

- Huebner, E. A. and Strittmatter, S. M. (2009). "Axon regeneration in the peripheral and central nervous systems." Results and Problems in Cell Differentiation **48**: 339-351.
- Joos, K. M., Li, C. and Sappington, R. M. (2010). "Morphometric changes in the rat optic nerve following short-term intermittent elevations in intraocular pressure." Investigative Ophthalmology and Visual Science **51**(12): 6431-6440.
- Kandel, E. R. (2013). Principles of Neural Science. New York, NY, McGraw Hill.
- Kim, J. E., Liu, B. P., Park, J. H. and Strittmatter, S. M. (2004). "Nogo-66 receptor prevents raphespinal and rubrospinal axon regeneration and limits functional recovery from spinal cord injury." Neuron **44**(3): 439-451.
- Kolb, H., Fernandez, E. and Nelson, R. (1995). Webvision: The Organization of the Retina and Visual System. Salt Lake City (UT), University of Utah Health Sciences Center.
- Korimova, A., Cížková, D., Toldi, J., Vécsei, L. and Vanický, I. (2012). "Protective effects of glucosamine-kynurenic acid after compression-induced spinal cord injury in the rat." Open Life Sciences **7**(6).
- Kuc, D., Zgrajka, W., Parada-Turska, J., Urbanik-Sypniewska, T. and Turski, W. A. (2008). "Micromolar concentration of kynurenic acid in rat small intestine." Amino Acids **35**(2): 503-505.
- Langner, E., Lemieszek, M. K., Kwiecień, J. M., Rajtar, G., Rzeski, W. and Turski, W. A. (2017). "Kynurenic Acid Induces Impairment of Oligodendrocyte Viability: On the Role of Glutamatergic Mechanisms." Neurochemical Research **42**(3): 838-845.
- Leaver, S. G., Cui, Q., Bernard, O. and Harvey, A. R. (2006). "Cooperative effects of bcl-2 and AAV-mediated expression of CNTF on retinal ganglion cell survival and axonal regeneration in adult transgenic mice." European Journal of Neuroscience **24**(12): 3323-3332.
- Leibinger, M., Müller, A., Andreadaki, A., Hauk, T. G., Kirsch, M. and Fischer, D. (2009). "Neuroprotective and axon growth-promoting effects following inflammatory stimulation on mature retinal ganglion cells in mice depend on ciliary neurotrophic factor and leukemia inhibitory factor." Journal of Neuroscience **29**(45): 14334-14341.
- Leon, S., Yin, Y., Nguyen, J., Irwin, N. and Benowitz, L. I. (2000). "Lens injury stimulates axon regeneration in the mature rat optic nerve." Journal of Neuroscience **20**(12): 4615-4626.
- Li, S., Liu, B. P., Budel, S., Li, M., Ji, B., Walus, L., Li, W., Jirik, A., Rabacchi, S., Choi, E., Worley, D., Sah, D. W., Pepinsky, B., Lee, D., Relton, J. and Strittmatter, S. M. (2004). "Blockade of Nogo-66, myelin-associated glycoprotein, and oligodendrocyte myelin glycoprotein by soluble Nogo-66 receptor promotes axonal sprouting and recovery after spinal injury." Journal of Neuroscience **24**(46): 10511-10520.

- Margalit, E. and Sadda, S. R. (2003). "Retinal and optic nerve diseases." Artificial Organs **27**(11): 963-974.
- Matute, C., Sánchez-Gómez, M. V., Martínez-Millán, L. and Miledi, R. (1997). "Glutamate receptor-mediated toxicity in optic nerve oligodendrocytes." Proceedings of the National Academy of Sciences of the United States of America **94**(16): 8830-8835.
- May, C. A. (2008). "Comparative Anatomy of the Optic Nerve Head and Inner Retina in Non- Primate Animal Models Used for Glaucoma Research." The Open Ophthalmology Journal **2**: 94-101.
- Mey, J. and Thanos, S. (2000). "Development of the visual system of the chick. I. Cell differentiation and histogenesis." Brain Research. Brain Research Reviews **32**(2-3): 343-379.
- Muller, A., Hauk, T. G. and Fischer, D. (2007). "Astrocyte-derived CNTF switches mature RGCs to a regenerative state following inflammatory stimulation." Brain **130**(Pt 12): 3308-3320.
- Muller, A., Hauk, T. G., Leibinger, M., Marienfeld, R. and Fischer, D. (2009). "Exogenous CNTF stimulates axon regeneration of retinal ganglion cells partially via endogenous CNTF." Molecular and Cellular Neuroscience **41**(2): 233-246.
- Nakazawa, T., Tachi, S., Aikawa, E. and Ihnuma, M. (1993). "Formation of the myelinated nerve fiber layer in the chicken retina." Glia **8**(2): 114-121.
- Nolte, J. (2009). The Human Brain: An Introduction to its Functional Anatomy. Philadelphia, PA, Mosby Elsevier.
- Ogawa, T., Matson, W. R., Beal, M. F., Myers, R. H., Bird, E. D., Milbury, P. and Saso, S. (1992). "Kynurenine pathway abnormalities in Parkinson's disease." Neurology **42**(9): 1702-1706.
- Ohshiro, H., Tonai-Kachi, H. and Ichikawa, K. (2008). "GPR35 is a functional receptor in rat dorsal root ganglion neurons." Biochemical and Biophysical Research Communications **365**(2): 344-348.
- Ohta, M., Ohta, K., Nishimura, M. and Saida, T. (2002). "Detection of myelin basic protein in cerebrospinal fluid and serum from patients with HTLV-1-associated myelopathy/tropical spastic paraparesis." Annals of Clinical Biochemistry **39**(Pt 6): 603-605.
- Oyster, C. W. (1999). The Human Eye: Structure and Function. Sunderland, MA, Sinauer Associates, Inc.
- Patel, A., Cholkar, K., Agrahari, V. and Mitra, A. K. (2013). "Ocular drug delivery systems: An overview." World Journal of Pharmacology **2**(2): 47-64.
- Purves, D., Augustine, G. J., Fitzpatrick, D., Katz, L. C., LaMantia, A., McNamara, J. O. and Williams, M., Eds. (2001). Neuroscience. Sunderland, MA, Sinauer Associates.

Quarles, R. H. (2007). "Myelin-associated glycoprotein (MAG): past, present and beyond." Journal of Neurochemistry **100**(6): 1431-1448.

Ramón y Cajal, S. (1995). Histology of the nervous system of man and vertebrates. New York, Oxford University Press.

Rejdak, K., Bartosik-Psujek, H., Dobosz, B., Kocki, T., Grieb, P., Giovannoni, G., Turski, W. A. and Stelmasiak, Z. (2002). "Decreased level of kynurenic acid in cerebrospinal fluid of relapsing-onset multiple sclerosis patients." Neuroscience Letters **331**(1): 63-65.

Rejdak, K., Petzold, A., Kocki, T., Kurzepa, J., Grieb, P., Turski, W. A. and Stelmasiak, Z. (2007). "Astrocytic activation in relation to inflammatory markers during clinical exacerbation of relapsing-remitting multiple sclerosis." Journal of Neural Transmission **114**(8): 1011-1015.

Richardson, P. M., McGuinness, U. M. and Aguayo, A. J. (1980). "Axons from CNS neurons regenerate into PNS grafts." Nature **284**(5753): 264-265.

Rogers, S. D. (2003). "Endothelin B receptors are expressed by astrocytes and regulate astrocyte hypertrophy in the normal and injured CNS." Glia **41**(2): 180-190.

Roymans, D., Vissenberg, K., De Jonghe, C., Grobden, B., Claes, P., Verbelen, J. P., Van Broeckhoven, C. and Slegers, H. (2001). "Phosphatidylinositol 3-kinase activity is required for the expression of glial fibrillary acidic protein upon cAMP-dependent induction of differentiation in rat C6 glioma." Journal of Neurochemistry **76**(2): 610-618.

Saito, K., Markey, S. P. and Heyes, M. P. (1992). "Effects of immune activation on quinolinic acid and neuroactive kynurenines in the mouse." Neuroscience **51**(1): 25-39.

Saito, K., Nowak, T. S., Jr., Suyama, K., Quearry, B. J., Saito, M., Crowley, J. S., Markey, S. P. and Heyes, M. P. (1993). "Kynurenine pathway enzymes in brain: responses to ischemic brain injury versus systemic immune activation." Journal of Neurochemistry **61**(6): 2061-2070.

Sapieha, P. S., Duplan, L., Uetani, N., Joly, S., Tremblay, M. L., Kennedy, T. E. and Di Polo, A. (2005). "Receptor protein tyrosine phosphatase sigma inhibits axon regrowth in the adult injured CNS." Molecular and Cellular Neuroscience **28**(4): 625-635.

Sapko, M. T., Guidetti, P., Yu, P., Tagle, D. A., Pellicciari, R. and Schwarcz, R. (2006). "Endogenous kynurenate controls the vulnerability of striatal neurons to quinolinate: Implications for Huntington's disease." Experimental Neurology **197**(1): 31-40.

Schwarcz, R. and Pellicciari, R. (2002). "Manipulation of brain kynurenines: glial targets, neuronal effects, and clinical opportunities." Journal of Pharmacology and Experimental Therapeutics **303**(1): 1-10.

Schwarcz, R., Rassoulpour, A., Wu, H. Q., Medoff, D., Tamminga, C. A. and Roberts, R. C. (2001). "Increased cortical kynurenate content in schizophrenia." Biological Psychiatry **50**(7): 521-530.

Siegel, G. J., Agranoff, B. W., Albers, R. W., Fisher, S. K. and Uhler, M. D. (1999). Basic Neurochemistry: Molecular, Cellular and Medical Aspects. Philadelphia, Lippincott-Raven.

Simonen, M., Pedersen, V., Weinmann, O., Schnell, L., Buss, A., Ledermann, B., Christ, F., Sansig, G., van der Putten, H. and Schwab, M. E. (2003). "Systemic deletion of the myelin-associated outgrowth inhibitor Nogo-A improves regenerative and plastic responses after spinal cord injury." Neuron **38**(2): 201-211.

Soto, A., Pérez-Samartín, A. L., Etxebarria, E. and Matute, C. (2004). "Excitotoxic insults to the optic nerve alter visual evoked potentials." Neuroscience **123**(2): 441-449.

Su, Y., Wang, F., Teng, Y., Zhao, S. G., Cui, H. and Pan, S. H. (2009). "Axonal regeneration of optic nerve after crush in Nogo66 receptor knockout mice." Neuroscience Letters **460**(3): 223-226.

Sun, D., Qu, J. and Jakobs, T. C. (2013). "Reversible reactivity by optic nerve astrocytes." Glia **61**(8): 1218-1235.

Tan, L., Yu, J. T. and Tan, L. (2012). "The kynurenine pathway in neurodegenerative diseases: mechanistic and therapeutic considerations." Journal of the Neurological Sciences **323**(1-2): 1-8.

Thomas, D. G., Palfreyman, J. W. and Ratcliffe, J. G. (1978). "Serum-myelin-basic-protein assay in diagnosis and prognosis of patients with head injury." Lancet **1**(8056): 113-115.

Thorburn, A. N., Macia, L. and Mackay, C. R. (2014). "Diet, metabolites, and "western-lifestyle" inflammatory diseases." Immunity **40**(6): 833-842.

Toosy, A. T., Mason, D. F. and Miller, D. H. (2014). "Optic neuritis." Lancet Neurology **13**(1): 83-99.

Trotter, J. L., Wegescheide, C. L. and Garvey, W. F. (1983). "Immunoreactive myelin proteolipid, protein-like activity in cerebrospinal fluid and serum of neurologically impaired patients." Annals of Neurology **14**(5): 554-558.

Uehara, M., Oomori, S., Kitagawa, H. and Ueshima, T. (1990). "The development of the pecten oculi in the chick." Nihon Juigaku Zasshi **52**(3): 503-512.

Vanezis, P., Chan, K. K. and Scholtz, C. L. (1987). "White matter damage following acute head injury." Forensic Science International **35**(1): 1-10.

Vidal-Sanz, M., Bray, G. M., Villegas-Perez, M. P., Thanos, S. and Aguayo, A. J. (1987). "Axonal regeneration and synapse formation in the superior colliculus by retinal ganglion cells in the adult rat." Journal of Neuroscience **7**(9): 2894-2909.

Wang, J., Simonavicius, N., Wu, X., Swaminath, G., Reagan, J., Tian, H. and Ling, L. (2006). "Kynurenic acid as a ligand for orphan G protein-coupled receptor GPR35." Journal of Biological Chemistry **281**(31): 22021-22028.

Weibel, D. (1994). "Regeneration of lesioned rat optic nerve fibers is improved after neutralization of myelin-associated neurite growth inhibitors." Brain Research **642**(1-2): 259-266.

Weinreb, R. N., Aung, T. and Medeiros, F. A. (2014). "The pathophysiology and treatment of glaucoma: a review." The Journal of the American Medical Association **311**(18): 1901-1911.

Whetsell, W. O., Jr. and Schwarcz, R. (1989). "Prolonged exposure to submicromolar concentrations of quinolinic acid causes excitotoxic damage in organotypic cultures of rat corticostriatal system." Neuroscience Letters **97**(3): 271-275.

Wiessner, C., Bareyre, F. M., Allegrini, P. R., Mir, A. K., Frentzel, S., Zurini, M., Schnell, L., Oertle, T. and Schwab, M. E. (2003). "Anti-Nogo-A antibody infusion 24 hours after experimental stroke improved behavioral outcome and corticospinal plasticity in normotensive and spontaneously hypertensive rats." Journal of Cerebral Blood Flow & Metabolism **23**(2): 154-165.

Yin, Y., Cui, Q., Li, Y., Irwin, N., Fischer, D., Harvey, A. R. and Benowitz, L. I. (2003). "Macrophage-derived factors stimulate optic nerve regeneration." Journal of Neuroscience **23**(6): 2284-2293.

Yiu, G. and He, Z. (2006). "Glial inhibition of CNS axon regeneration." Nature Reviews. Neuroscience **7**(8): 617-627.

Zadori, D., Nyiri, G., Szonyi, A., Szatmári, I., Fülöp, F., Toldi, J., Freund, T. F., Vécsei, L. and Klivényi, P. (2011). "Neuroprotective effects of a novel kynurenic acid analogue in a transgenic mouse model of Huntington's disease." Journal of Neural Transmission **118**(6): 865-875.

Zhou, J. B., Ge, S., Gu, P., Peng, D., Chen, G. F., Pan, M. Z. and Qu, J. (2011). "Microdissection of guinea pig extraocular muscles." Experimental and Therapeutic Medicine **2**(6): 1183-1185.

Zinger, A., Barcia, C., Herrero, M. T. and Guillemin, G. J. (2011). "The involvement of neuroinflammation and kynurenine pathway in Parkinson's disease." Parkinson's Disease **2011**: 716859.